

Supporting Information

Controlling the Rectification Properties of Molecular Junctions through Molecule–Electrode Coupling

Matthieu Koepf, Christopher Koenigsmann, Wendu Ding, Arunbah Batra, Christian F.A. Negre, Latha Venkataraman, Gary W. Brudvig, Victor S. Batista, Charles A. Schmuttenmaer, and Robert H. Crabtree

Content

1. Synthesis and characterization of the <i>N</i> -phenylbenzamide (NPBA) derivatives	4
1.1 Reagents, solvents and glassware handling	4
1.2 Experimental procedures	5
2. Theoretical studies.....	14
2.1 Description of the leads	14
2.2 Representation of the density of State (DOS) for the different junctions	15
2.3 Representation of the eigenchannel computed at E_{NPBA} for each junction	16
2.4 Representation of the HOMO state distribution for the isolated NPBA backbone	16
2.5 Single-state tight-binding model	17
2.6 Angular dependence of the projected density of states of the phenyl and the Anchor-leads fragments $PDOS_{Ph}/PDOS_{Au-Anchor}$	19
3. NMR spectra	21
3.1 1H NMR spectra of 4'-methyl- <i>N</i> -methyl- <i>N</i> -(4-tolyl)benzamide in $CDCl_3$	21
3.2 ^{13}C NMR spectra of 4'-methyl- <i>N</i> -methyl- <i>N</i> -(4-tolyl)benzamide in $CDCl_3$	22
3.3 1H NMR spectra of 4'-bromomethyl- <i>N</i> -methyl- <i>N</i> -[4-(bromomethyl)phenyl]benzamide in CD_3CN	23
3.4 ^{13}C NMR spectra of 4'-bromomethyl- <i>N</i> -methyl- <i>N</i> -[4-(bromomethyl)phenyl]benzamide in CD_3CN	24
3.5 1H NMR spectra of 4'-(trimethylstannyl)methyl- <i>N</i> -methyl- <i>N</i> -[4((trimethylstannyl)-methylphenyl)]benzamide in CD_3OD	25
3.6 ^{13}C NMR spectra of 4'-(trimethylstannyl)methyl- <i>N</i> -methyl- <i>N</i> -[4((trimethylstannyl)-methylphenyl)]benzamide in CD_3OD	26
3.7 1H NMR spectra of 2[-4-(2',2',2'-trifluoroacetamido)phenyl]ethan-1-ol in $CDCl_3$	27
3.8 ^{19}F NMR spectra of 2[-4-(2',2',2'-trifluoroacetamido)phenyl]ethan-1-ol in $CDCl_3$	28
3.9 ^{13}C NMR spectra of 2[-4-(2',2',2'-trifluoroacetamido)phenyl]ethan-1-ol in $CDCl_3$	29
3.10 1H NMR spectra of 2,2,2-trifluoro-(4-(2-((tetrahydro-2 <i>H</i> -pyran-2-yl)oxy)ethyl)phenyl)acetamide in $CDCl_3$	30
3.11 ^{19}F NMR spectra of 2,2,2-trifluoro-(4-(2-((tetrahydro-2 <i>H</i> -pyran-2-yl)oxy)ethyl)phenyl)acetamide in $CDCl_3$	31
3.12 ^{13}C NMR spectra of 2,2,2-trifluoro-(4-(2-((tetrahydro-2 <i>H</i> -pyran-2-yl)oxy)ethyl)phenyl)acetamide in $CDCl_3$	32
3.13 1H NMR spectra of 2,2,2-trifluoro- <i>N</i> -methyl-(4-(2-((tetrahydro-2 <i>H</i> -pyran-2-yl)oxy)ethyl)-phenyl)acetamide in $CDCl_3$	33
3.14 ^{19}F NMR spectra of 2,2,2-trifluoro- <i>N</i> -methyl-(4-(2-((tetrahydro-2 <i>H</i> -pyran-2-yl)oxy)ethyl)-phenyl)acetamide in $CDCl_3$	34
3.15 ^{13}C NMR spectra of 2,2,2-trifluoro- <i>N</i> -methyl-(4-(2-((tetrahydro-2 <i>H</i> -pyran-2-yl)oxy)ethyl)-phenyl)acetamide in $CDCl_3$	35
3.16 1H NMR spectra of <i>N</i> -methyl-(4-(2-((tetrahydro-2 <i>H</i> -pyran-2-yl)oxy)ethyl)aniline in $CDCl_3$..	36

3.17 ¹³ C NMR spectra of <i>N</i> -methyl-4-(2-((tetrahydro-2 <i>H</i> -pyran-2-yl)oxy)ethyl)aniline in CDCl ₃	37
3.18 ¹ H NMR spectra of 4-(2-bromoethyl)- <i>N</i> -methyl- <i>N</i> -(4-(2-((tetrahydro-2 <i>H</i> -pyran-2-yl)oxy)ethyl)phenyl)benzamide in CDCl ₃	38
3.19 ¹³ C NMR spectra of 4-(2-bromoethyl)- <i>N</i> -methyl- <i>N</i> -(4-(2-((tetrahydro-2 <i>H</i> -pyran-2-yl)oxy)ethyl)phenyl)benzamide in CDCl ₃	39
3.20 ¹ H NMR spectra of 4-(2-bromoethyl)- <i>N</i> -methyl- <i>N</i> -(4-(2-bromoethyl)phenyl)benzamide in CDCl ₃	40
3.21 ¹³ C NMR spectra of 4-(2-bromoethyl)- <i>N</i> -methyl- <i>N</i> -(4-(2-bromoethyl)phenyl)benzamide in CDCl ₃	41
3.22 ¹ H NMR spectra of 4-(trimethylstannyl)ethyl- <i>N</i> -methyl- <i>N</i> -(4 ((trimethylstannyl)ethyl)phenyl)benzamide	42
3.23 ¹³ C NMR spectra of 4-(trimethylstannyl)ethyl- <i>N</i> -methyl- <i>N</i> -(4 ((trimethylstannyl)ethyl)phenyl)benzamide	43
4. References	44

1. Synthesis and characterization of the *N*-phenylbenzamide (NPBA) derivatives

1.1 Reagents, solvents and glassware handling

p-Tolylchloride, *N,N*-diisopropylethylamine, *N*-methyl-*p*-toluidine, *N*-bromosuccinimide, hexamethyldistannane, trifluoroacetic anhydride, *p*-toluenesulfonic acid, sodium hydride (60 wt-% dispersed in mineral oil), methyl iodide, ammonium chloride, oxalyl chloride, carbon tetrabromide, triphenylphosphine, and *n*-butyllithium (2.1M in hexanes) (reagents purity: 97-% or higher) were obtained from Alfa Aesar. 4-(*N,N*-dimethylamino)pyridine, triethylamine, 3,4-dihydro-2*H*-pyran and anhydrous potassium carbonate (K₂CO₃) (reagents purity: 97-% or higher) were obtained from Acros Organics. *Tetrakis*(triphenylphosphine)palladium(0), and copper(I)cyanide were purchased from Strem Chemicals. Benzoyl peroxide was purchased from Aldrich. 2-(Aminophenyl)ethanol was obtained from TCI America. All the reagents were used as received. For synthetic purposes dichloromethane (CH₂Cl₂, OmniSolv grade, EMD-Millipore) and tetrahydrofuran (THF, OmniSolv grade, non-stabilized, EMD-Millipore) were dried on a Pure Solv MD-5 solvent purification system (Innovative Technology) on activated aluminum oxide before use and were dispensed under nitrogen. Anhydrous benzene (Alfa Aesar DriSolv), methanol (MeOH, ACS grade, BDH), 200 proof ethanol (EtOH, Decon labs), and dimethylformamide (DMF, DriSolv grade, EMD-Millipore) were used as received. *N,N*-Diisopropylethylamine (DIPEA) and triethylamine (NEt₃) were distilled over potassium hydroxide (KOH) and stored under argon (Ar) before use. The glassware was oven-dried and cooled under nitrogen prior use. Anhydrous sodium sulfate (Na₂SO₄), sodium bicarbonate (NaHCO₃), citric acid, and sodium chloride (ACS grade) were obtained from JT-Baker. For purification purposes, dichloromethane (CH₂Cl₂, ACS grade, stabilized with amylenes, BDH), ethyl acetate (EtOAc, ACS grade, BDH), methanol (MeOH, ACS grade, BDH), hexanes (ACS grade, BDH) as well as toluene (ACS grade, Macron Fine Chemicals) were used

without further purification. For nuclear magnetic resonance studies (NMR), deuterated acetonitrile (CD₃CN containing 0.05 v/v-% of tetramethylsilane (TMS)), deuterated methanol (CD₃OD) and deuterated chloroform (CDCl₃, containing 0.05% v/v-% TMS) were obtained from Cambridge Isotope Laboratory.

Analytical thin layer chromatography (TLC) was conducted on glass-coated silica gel 60 F254 plates obtained from EMD-Millipore. Column chromatography were conducted on silica gel (SiO₂, 43–60 μm or 18–22 μm) provided by Silicycle. Unless otherwise specified, the 43–60 μm silica gel was used as stationary phase for the columns. Celite® 545 was purchased from EMD-Millipore. NMR spectra were recorded on a Varian DPX spectrometer coupled to an Oxford 400 magnet. ¹H spectra were recorded at 400 MHz, and ¹³C NMR at 101 MHz. Chemical shifts are reported according to TMS as the internal reference. High resolution mass spectrometry was performed on an Agilent G6550A Q-TOF LC/MS with API by direct injection, otherwise the sample were run on a an Agilent-1260 Infinity(LC)/6120B(MS) system using a C18 column (1.8 μm, 4.6 x 50 mm); in all cases the compounds were dissolved in methanol at an approximate concentration of 0.5 mg/mL. All the NPBA derivatives were stored under Ar at -20°C.

1.2 Experimental procedures

Synthesis and full characterization of NH₂-NPBA derivative has been described elsewhere.¹

Synthesis of 4'-methyl-N-methyl-N-(4-tolyl)benzamide

p-Tolylchloride (4.78 g, 30.9 mmol) was dissolved in anhydrous dichloromethane (40 mL). *N,N*-dimethyl-4-aminopyridine (0.62 g, 5.15 mmol) and dry *N,N*-diisopropylethylamine (6.9 ml, 5.16 g, 40 mmol) were added under nitrogen. *N*-Methyl-*p*-toluidine (2.6 mL, 2.5 g, 20.6 mmol) was added dropwise over a period of 5 minutes and the mixture was refluxed under nitrogen for 2 hours. TLC analysis (SiO₂, CH₂Cl₂) indicated that all the *N*-methyl-*p*-toluidine was converted. The mixture was extracted with 5% aqueous NaHCO₃ (2 x 100 mL), 5% aqueous citric acid (2 x 100 mL) and water (100 mL). The organic layer was dried over

Na₂SO₄, filtered, and the solvent was evaporated. Column chromatography (SiO₂, CH₂Cl₂ 1%- EtOAc) yielded the desired product as an off-white solid (5.01 g, 20.1 mmol, 98%).

¹H-NMR (400 MHz, CDCl₃) δ 7.20 (d, *J* = 8.1 Hz, 2H), 7.02 (d, *J* = 8.0 Hz, 2H), 6.96 (d, *J* = 8.0 Hz, 2H), 6.91 (d, *J* = 8.3 Hz, 2H), 3.45 (s, 3H), 2.28 (s, 3H), 2.26 (s, 3H).

¹³C-NMR (101 MHz, CDCl₃) δ 170.63, 142.62, 139.59, 136.09, 133.06, 129.71, 128.84, 128.30, 126.61, 38.56, 21.31, 20.93.

MS (m/z 100%) calc. for C₁₆H₁₇NO+H⁺: 240.1; found 240.2.

Synthesis of 4'-bromomethyl-*N*-methyl-*N*-[4-(bromomethyl)phenyl]benzamide

4-methyl-*N*-methyl-*N*-(4-tolyl)benzamide (2g, 8.56 mmol) was dissolved in anhydrous benzene (10 mL) under nitrogen. The mixture was purged with nitrogen (vacuum-nitrogen cycles, 3x) and brought to 80 °C under nitrogen. *N*-bromosuccinimide (2.97 g, 16.72 mmol) and benzoyl peroxide (387 mg, 1.6 mmol) were added and the mixture was stirred under gentle reflux for 1 hour under nitrogen. TLC analysis (SiO₂, toluene 5%-EtOAc) indicated full conversion of the starting material. The solution was cooled down to room temperature and the solid filtered out and washed with toluene (3 x 30 mL). The solvent was evaporated and the crude was purified by column chromatography (SiO₂ hexanes-20% EtOAc, 5th band collected). The obtained product contained a minor impurity that was eliminated by running a second column chromatography (SiO₂, CH₂Cl₂ 1%-EtOAc, 2nd band collected). The desired compound was obtained as a white solid (1.5 g, 3.78 mmol, 44%).

¹H-NMR (400 MHz, CD₃CN) δ 7.31 (d, *J* = 8.4 Hz, 2H), 7.27 (br s, 4H), 7.12 (d, *J* = 8.4 Hz, 2H), 4.51 (s, 2H), 4.49 (s, 2H), 3.38 (s, 3H).

¹³C-NMR (101 MHz, CD₃CN) δ 169.49, 144.85, 139.67, 136.65, 129.86, 128.82, 128.51, 127.45, 37.62, 32.81, 32.70.

MS (m/z 100%) calc. for C₁₆H₁₅Br₂NO+H⁺: 397.9; found 397.8.

Synthesis of 4'-(trimethylstannyl)methyl-*N*-methyl-*N*-[4((trimethylstannyl)methylphenyl)]benzamide

4'-bromomethyl-*N*-methyl-*N*-[4-(bromomethyl)phenyl]benzamide (199 mg, 0.5 mmol) and melted hexamethyldistannane (0.4 mL, 632 mg, 1.9 mmol) were dissolved in anhydrous toluene (20 mL) and the mixture was purged with argon (vacuum/argon cycles, 3x). Tetrakis(triphenylphosphine)palladium(0) (12 mg, 10 μ mol) was added and the mixture purged with argon (vacuum/argon cycles, 3x) and stirred at 90 °C under argon for 12 hours. TLC analysis (SiO₂, CH₂Cl₂-2% EtOAc) indicated that the reaction was complete. The mixture was filtered over Celite® to remove the precipitated solid and the solvent was evaporated. The crude material was purified by column chromatography (SiO₂, CH₂Cl₂-1% EtOAc). The second band contained the desired product. It was collected and the solvent was evaporated. A second column chromatography (SiO₂ hexanes-20% EtOAc) yielded the pure 4'-(trimethylstannyl)methyl-*N*-methyl-*N*-[4((trimethylstannyl)methylphenyl)] benzamide (second product collected) as a white solid (176 mg, 0.31 mmol, 62%).

¹H-NMR (400 MHz, CD₃OD) δ 7.08 (d, J = 8.3 Hz, 2H), 6.95 – 6.82 (m, 4H), 6.78 (d, J = 7.8 Hz, 2H), 3.41 (s, 3H), 2.40 – 2.12 (m, 4H), 0.20 – -0.21 (m, 18H).

¹³C-NMR (101 MHz, CD₃OD) δ 171.79, 146.06, 142.37, 140.06, 130.28, 128.60, 126.98, 126.57, 125.54, 37.41, 19.73, 19.00, -11.68, -11.72.

HRMS (m/z 100%) calc. for C₂₂H₃₃NOSn₂+H⁺: 566.0673; found 566.0670.

Synthesis of 2-[4-(2',2',2'-trifluoroacetamido)phenyl]ethyl-2'',2'',2''-trifluoroacetate

2-(4-aminophenyl)ethanol (288 mg, 2.1 mmol) was dissolved in anhydrous dichloromethane (50 mL). K₂CO₃ (1.38 g, 10 mmol) was added followed by trifluoroacetic anhydride (0.84 mL, 1.26 g, 6 mmol) and the mixture was stirred at room temperature, under nitrogen for 1 hour. TLC analysis (SiO₂, CH₂Cl₂) confirmed that the reaction was complete and the mixture was filtered to remove the solid. The organic layer was washed with water (3

x 50 mL), collected dried on Na₂SO₄ filtered and the solvent was evaporated to yield the desired compound as a white solid (635 mg, 1.9 mmol, 92%). The compound was used for the next step without further purification.

Due to the fast hydrolysis of the trifluoroacetate ester, traces of the free alcohol were observed in NMR spectroscopy.

Synthesis of 2[-4-(2',2',2'-trifluoroacetamido)phenyl]ethan-1-ol

2-[4-(2',2',2'-trifluoroacetamido)phenyl]ethyl-2'',2'',2''-trifluoroacetate (635 mg, 1.9 mmol) was dissolved in methanol (50 mL) and 9 μ L of a 2.3 M aqueous solution of potassium hydroxide (20 μ mol) was added and the mixture was stirred at 50 °C, under nitrogen, for 1 hour. TLC analysis (SiO₂, hexanes-20% EtOAc) confirmed the full conversion of the starting material. The solution was cooled down to room temperature, and the solvent was evaporated under reduced pressure to yield the desired product as a white solid (446 mg, quant.). It was used for the next reaction without further purification.

¹H NMR (400 MHz, CDCl₃) δ 7.86 (br. s, 1H), 7.51 (d, J = 8.5 Hz, 2H), 7.25 (d, J = 8.5 Hz, 2H), 3.86 (t, J = 6.5 Hz, 2H), 2.88 (t, J = 6.5 Hz, 2H).

¹⁹F NMR (376 MHz, CDCl₃) δ -75.72.

¹³C NMR (101 MHz, CDCl₃) δ 136.95, 133.44, 129.91, 120.70, 63.45, 38.57.

MS analysis did not show the expected molecular ion of the alcohol derivative (C₁₀H₁₀F₃NO₂+H⁺) but the product of acid catalyzed dehydration was observed:

MS (m/z 100%) calc. for C₁₀H₈F₃NO+H⁺: 248.1; found 248.0.

Synthesis of 2,2,2-trifluoro-(4-(2-((tetrahydro-2H-pyran-2-yl)oxy)ethyl)phenyl)acetamide

2[-4-(2',2',2'-trifluoroacetamido)phenyl]ethan-1-ol was dissolved in anhydrous dichloromethane (50 mL), 3,4-dihydro-2H-pyran (200 μ L, 192 mg, 2.28 mmol) was added followed by *p*-toluenesulfonic acid (19 mg, 0.1 mmol). The mixture was stirred under nitrogen, at room temperature. After 4 hours, TLC analysis (SiO₂, hexanes-10% EtOAc)

indicated full conversion of the starting material. The mixture was extracted with 5%-aqueous NaHCO₃ (2 x 50 mL) and water (1 x 50 mL). The organic layer was collected, dried over Na₂SO₄, filtered and the solvent was evaporated under reduced pressure. The crude residue was purified by column chromatography (SiO₂, hexanes-10% EtOAc) to yield the desired compound as a clear oil (655.2 mg, 2.06 mmol, 91%).

¹H NMR (400 MHz, CDCl₃) δ 7.84 (br. s, 1H), 7.48 (d, *J* = 8.5 Hz, 2H), 7.27 (d, *J* = 8.5 Hz, 2H), 4.58 (dd, *J*₁ = 4.2 Hz, *J*₂ = 2.8 Hz, 1H), 3.94 (dt, *J*₁ = 9.7 Hz, *J*₂ = 7.0 Hz, 1H), 3.77 – 3.71 (m, 1H), 3.60 (dt, *J*₁ = 9.7 Hz, *J*₂ = 6.9 Hz, 1H), 3.48 – 3.43 (m, 1H), 2.90 (t, *J* = 7.0 Hz, 2H), 1.82 – 1.72 (m, 1H), 1.75 – 1.64 (m, 1H), 1.63 – 1.42 (m, 4H).

¹⁹F NMR (376 MHz, CDCl₃) δ -75.73.

¹³C NMR (101 MHz, CDCl₃) δ 137.67, 133.15, 129.88, 120.37, 98.75, 67.92, 62.19, 35.79, 30.62, 25.41, 19.45.

MS (m/z 100%) calc. for C₁₅H₁₈F₃NO₃+Na⁺: 340.1; found 340.0.

Synthesis of 2,2,2-trifluoro-*N*-methyl-(4-(2-((tetrahydro-2*H*-pyran-2-yl)oxy)ethyl) phenyl acetamide

2,2,2-trifluoro-(4-(2-((tetrahydro-2*H*-pyran-2-yl)oxy)ethyl)phenyl)acetamide (607 mg, 1.9 mmol) was dissolved in anhydrous THF (25 mL) under nitrogen. sodium hydride (60 wt-% dispersion in mineral oil, 87 mg, 2.18 mmol) was added and the reaction mixture was stirred under nitrogen, at room temperature, for 5 minutes. Methyl iodide (200 μL, 456 mg, 3.2 mmol) was added and the mixture was stirred at 45 °C, under nitrogen. The progression of the reaction was followed by TLC analysis (SiO₂, hexanes-10% EtOAc). After 2 hours complete conversion of the starting material was observed. The mixture was cooled down to room temperature and quenched with a saturated solution of aqueous ammonium chloride (1 mL). The mixture was poured into a 5% aqueous NaHCO₃ solution (100 mL). The aqueous layer was extracted with ethyl acetate (2 x 50 mL). The combined organic layers were then washed

with a 5% aqueous solution of NaHCO₃ (100 mL) and water (100 mL). The organic layer was collected, dried over Na₂SO₄, filtered and the solvent was evaporated under reduced pressure. Column chromatography (SiO₂, hexanes-10% EtOAc) yield the desired compound as a colorless oil. ¹H-NMR showed that it was 90% pure containing some *N,N*-dimethyl-(4-(2-((tetrahydro-2*H*-pyran-2-yl)oxy)ethyl)aniline. It was use without further purification in the next step. Yield: 591 mg, 1.78 mmol, 94%.

¹H NMR (400 MHz, CDCl₃) δ 7.31 (d, *J* = 8.3 Hz, 2H), 7.15 (d, *J* = 8.3 Hz, 2H), 4.60 – 4.58 (m, 1H), 3.94 (dt, *J*₁ = 9.7 Hz, *J*₂ = 7.0 Hz, 1H), 3.66 – 3.60 (m, 2H), 3.52 – 3.39 (m, 1H), 3.34 (s, 3H), 2.94 (t, *J* = 7.0 Hz, 2H), 1.88 – 1.63 (m, 2H), 1.63 – 1.43 (m, 4H).

¹⁹F NMR (376 MHz, CDCl₃) δ -67.10.

¹³C NMR (101 MHz, CDCl₃) δ 140.56, 130.11, 127.09, 98.55, 67.60, 61.98, 39.69, 35.91, 30.57, 29.68, 25.38, 19.31.

MS (m/z 100%) calc. for C₁₆H₂₀F₃NO₃+H⁺: 332.2; found 332.2.

Synthesis of *N*-methyl-(4-(2-((tetrahydro-2*H*-pyran-2-yl)oxy)ethyl)aniline

2,2,2-trifluoro-*N*-methyl- (4-(2-((tetrahydro-2*H*-pyran-2-yl)oxy)ethyl)phenylacetamide (570 mg, 1.72 mmol) was dissolved in methanol (25 mL). Potassium hydroxide (250 mg, 4.45 mmol) dissolved in 1 mL of water was added and the mixture was purged with nitrogen (vacuum nitrogen cycles, 3x). The mixture was stirred at room temperature, under nitrogen, for 3 hours. TLC analysis (SiO₂, toluene-10% EtOAc) indicated complete conversion of the starting material. The solvent was evaporated to 5 mL and the mixture diluted to 50 mL with EtOAc. The organic layer was extracted with brine (3 x 50 mL), collected, dried over Na₂SO₄, filtered and the solvent was evaporated to yield the desired aniline as a colorless oil (404 mg, 1.72 mmol, quant.). The aniline was used without further purification in the following step.

¹H NMR (400 MHz, CDCl₃) δ 7.06 (d, *J* = 8.4 Hz, 2H), 6.56 (d, *J* = 8.4 Hz, 2H), 4.59 (dd, *J*₁ = 4.4 Hz, *J*₂ = 2.9 Hz, 1H), 3.89 (dt, *J*₁ = 9.7 Hz, *J*₂ = 7.4 Hz, 1H), 3.82 – 3.78 (m, 1H), 3.56 (dt, *J*₁ = 9.7 Hz, *J*₂ = 7.4 Hz, 1H), 3.51 – 3.42 (m, 1H), 2.82 (s, 3H), 2.81 (t, *J* = 7.0 Hz, 2H), 1.88 – 1.77 (m, 1H), 1.76 – 1.64 (m, 1H), 1.64 – 1.44 (m, 4H).

¹³C NMR (101 MHz, CDCl₃) δ 147.66, 129.68, 127.68, 112.52, 98.73, 68.83, 62.24, 35.45, 30.99, 30.72, 25.49, 19.58.

MS (m/z 100%) calc. for C₁₄H₂₁NO₂+H⁺: 236.2; found 236.2.

Synthesis of 4-(2-bromoethyl)-*N*-methyl-*N*-(4-(2-((tetrahydro-2*H*-pyran-2-yl)oxy)ethyl)-phenyl)benzamide

4-(2-bromoethyl)benzoic acid (690 mg, 3mmol) was suspended in anhydrous benzene (30 mL) under nitrogen. Oxalyl chloride (326 μL, 474 mg, 3.75 mmol) was added followed by a drop of anhydrous dimethylformamide (5 μL). The mixture was stirred at room temperature, under nitrogen for 3 hours. The solvent was reduced to 10 mL and anhydrous triethylamine (1.2 mL, 0.859 mg, 8.5 mmol) was added, followed by a solution of *N*-methyl-(4-(2-((tetrahydro-2*H*-pyran-2-yl)oxy)ethyl)aniline (400 mg, 1.7 mmol) in anhydrous dichloromethane (6 mL) and *N,N*-dimethylaminopyridine (25 mg, 0.2 mmol). The mixture was further stirred under nitrogen, at room temperature for 12 hours. The mixture was diluted to 100 mL with dichloromethane and extracted with 5% aqueous NaHCO₃ (2 x 100 mL) and water (100 mL). The organic layer was collected, dried over Na₂SO₄, filtered and the solvent was evaporated. The crude residue was purified by column chromatography (SiO₂, CH₂Cl₂-6% EtOAc) to yield the desired compound as a colorless oil (618 mg, 1.3 mmol, 81%).

¹H NMR (400 MHz, CDCl₃) δ 7.25 (d, *J* = 8.1 Hz, 2H), 7.10 (d, *J* = 8.3 Hz, 2H), 7.00 (d, *J* = 8.1 Hz, 2H), 6.94 (d, *J* = 8.3 Hz, 2H), 4.56 – 4.54 (m, 1H), 3.88 (dt, *J*₁ = 9.7 Hz, *J*₂ = 7.1 Hz, 1H), 3.75 – 3.69 (m, 1H), 3.55 (dt, *J*₁ = 9.7 Hz, *J*₂ = 7.0 Hz, 1H), 3.52 – 3.39 (m, 6H), 3.07 (t, *J* = 7.6 Hz, 2H), 2.84 (t, *J* = 7.1 Hz, 2H), 1.80 – 1.75 (m, 1H), 1.70 – 1.65 (m, 1H), 1.58 – 1.48 (m, 4H).

¹³C NMR (101 MHz, CDCl₃) δ 170.29, 142.99, 140.34, 137.63, 134.61, 129.71, 129.08, 127.95, 126.63, 98.70, 67.91, 62.17, 39.03, 38.50, 35.74, 32.20, 30.60, 25.41, 19.45.

MS (m/z 100%) calc. for C₂₃H₂₈BrNO₃+H⁺: 446.1; found 446.0.

Synthesis of 4-(2-bromoethyl)-*N*-methyl-*N*-(4-(2-bromoethyl)phenyl)benzamide

4-(2-bromoethyl)-*N*-methyl-*N*-(4-(2-((tetrahydro-2*H*-pyran-2-yl)oxy)ethyl)phenyl)benzamide (100 mg, 0.22 mmol) was dissolved in anhydrous dichloromethane (2.5 mL), carbon tetrabromide (97 mg, 0.29 mmol) was added and the mixture stirred at room temperature, under nitrogen, for 10 minutes before being cooled down to 0 °C. Triphenylphosphine (153 mg, 0.58 mmol) was added and the mixture was stirred at 0 °C, under nitrogen, for 1 hour then allowed to warm up to room temperature. The mixture was further stirred at room temperature for 2 hours after which time TLC analysis (SiO₂, CH₂Cl₂-10% EtOAc) showed that all the starting material reacted. The crude mixture was purified by column chromatography (SiO₂, CH₂Cl₂-10% EtOAc) to yield the desired product as a colorless oil (93 mg, 0.22 mmol, 98%).

¹H NMR (400 MHz, CDCl₃) δ 7.24 (d, *J* = 8.1 Hz, 2H), 7.07 (d, *J* = 8.3 Hz, 2H), 7.01 (d, *J* = 8.2 Hz, 2H), 6.98 (d, *J* = 8.3 Hz, 2H), 3.52 – 3.44 (m, 7H), 3.11 – 3.05 (m, 4H).

¹³C NMR (101 MHz, CDCl₃) δ 170.27, 143.63, 140.45, 137.16, 134.45, 129.39, 129.08, 128.01, 126.93, 38.99, 38.56, 38.37, 32.67, 32.31.

MS (m/z 100%) calc. for C₁₈H₁₉Br₂NO+H⁺: 426.0; found 426.0.

Synthesis of 4-(trimethylstannyl)ethyl-*N*-methyl-*N*-(4-((trimethylstannyl)ethyl)phenyl)benzamide

Copper cyanide (68 mg, 0.76 mmol) was suspended in oxygen free, anhydrous THF. The suspension was purged with argon (vacuum argon cycles, 3 cycles) and cooled down to -40 °C using an acetonitrile-dry ice cooling bath. *n*-Buthyllithium (680 μ L, 2.2 M in hexanes, 0.15mmol) was added dropwise to the suspension and the mixture was stirred at -40 °C for 30 minutes, under argon. Hexamethyldistannane (146 μ L, 231 mg, 0.71 mmol) was added dropwise and the mixture was further stirred at -40 °C for 1 hour under argon. The cuprate solution was then cooled down to -78 °C (acetone/dry ice bath) and an oxygen-free solution of 4-(2-bromoethyl)-*N*-methyl-*N*-(4-(2-bromoethyl)phenyl)benzamide (100 mg, 0.23 mmol) dissolved in anhydrous THF (5 mL) was transferred dropwise to the cold cuprate slurry (addition time ca. 5 minutes) via a cannula. The mixture was further stirred at -78 °C for 15 minutes, then stirred at -40 °C for 15 minutes and was then slowly allowed to warm up to 0 °C and stirred at 0 °C, another 30 minutes, under argon. The reaction was quenched with a saturated aqueous solution of ammonium chloride (5 mL). The mixture was poured into hexanes (100 mL) and the organic phase was then washed with saturated aqueous ammonium chloride (2 x 50 mL) and water (1 x 50 mL). The organic layer was collected, dried over Na₂SO₄, filtered and the solvent was evaporated. The crude residue was purified by column chromatography (SiO₂, 18 – 22 μ m, toluene-5% EtOAc) to yield the desired compound (32.1 mg, 54 μ mol, 23%, first eluted band) as a white solid.

¹H NMR (400 MHz, CDCl₃) δ 7.22 (d, *J* = 7.9 Hz, 2H), 7.03 (d, *J* = 8.1 Hz, 2H), 6.97 (d, *J* = 8.0 Hz, 2H), 6.93 (d, *J* = 8.1 Hz, 2H), 3.46 (s, 3H), 2.91 – 2.54 (m, 4H), 1.08 (h, *J* = 7.7 Hz, 4H), 0.23 – -0.32 (m, 18H).

¹³C NMR (101 MHz, CDCl₃) δ 170.64, 146.83, 143.36, 142.84, 133.27, 129.02, 128.51, 127.15, 126.68, 38.59, 32.36, 32.01, 12.21, 12.03, -10.21.

HRMS (m/z 100%) calc. for C₂₄H₃₇NOSn₂+H⁺: 594.0986; found 594.0986.

2. Theoretical studies

2.1 Description of the leads

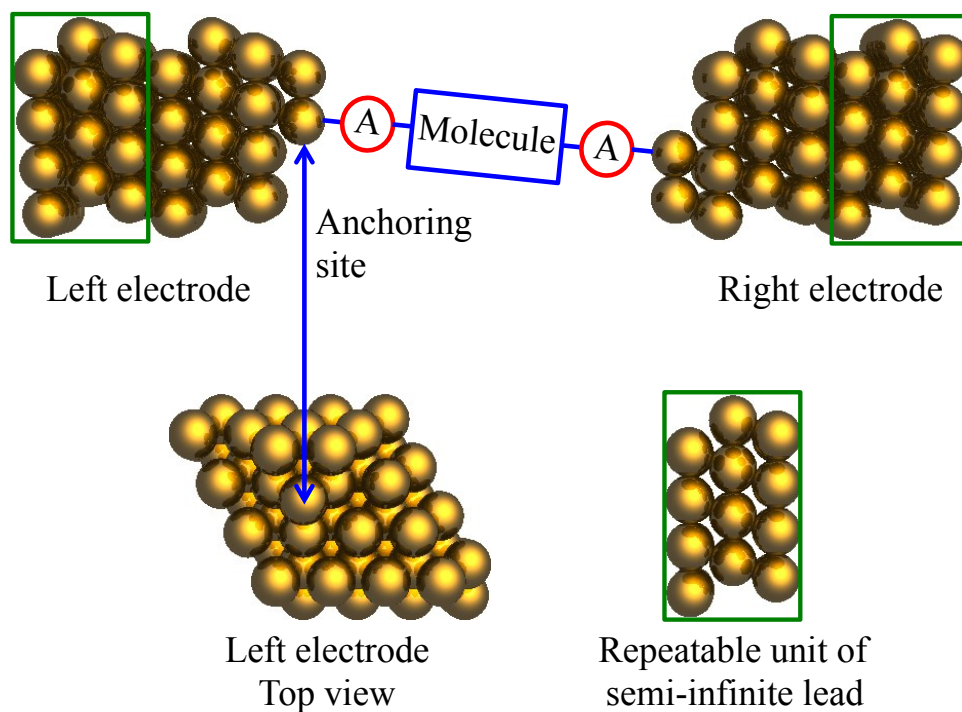


Figure S1. Representation of the gold electrodes used in I-V curve calculations. They consist of 6 layers of 16 gold atoms cut from an Au fcc lattice, with a triad contact motif attached to the (111) surface. The lattice constant is 4.080 Å.

2.2 Representation of the density of State (DOS) for the different junctions

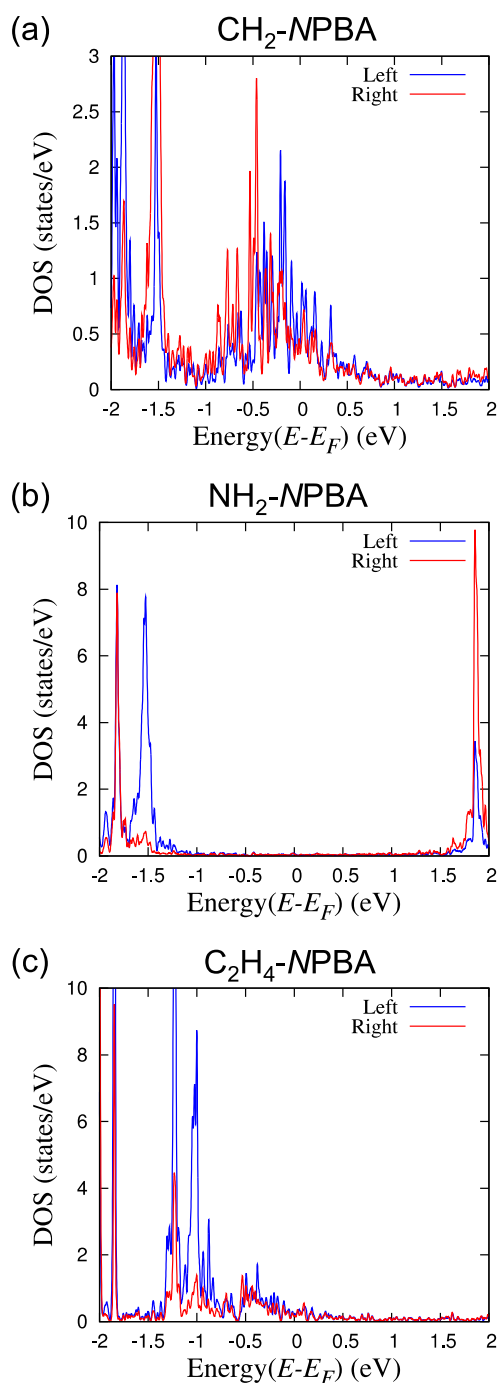


Figure S2. Representation of the density of states for all three molecules. Blue line (labeled Left) indicates states localized on the left-hand side of the molecule, while red line (labeled Right) indicates states localized on the right-hand side of the molecule. Left and right sides are determined with respect to the central amide bond and systematically using the -PhNMeCOPh- orientation.

2.3 Representation of the eigenchannel computed at E_{NPBA} for each junction

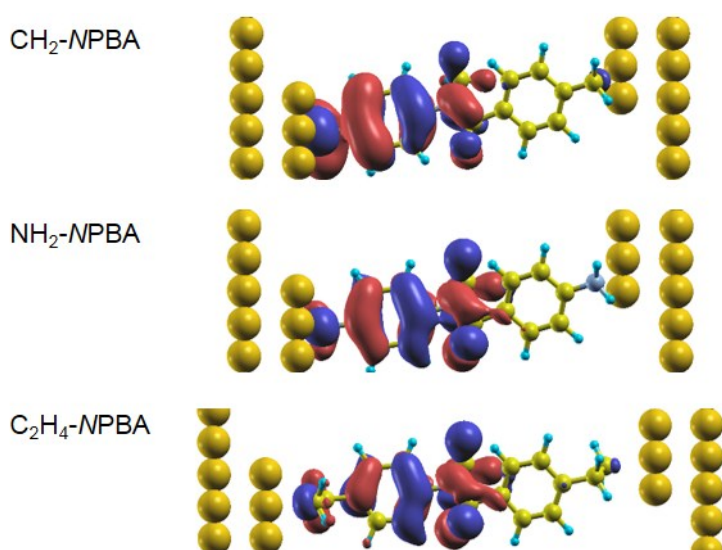


Figure S3. Representation of the eigenchannel at E_{NPBA} for each junction. Note the clear homology between the eigenchannels of the three junctions. Since the eigenchannel represents the principal eigenvector of the transmission matrix it gives a picture of the orbitals involved in the electron transport through the junction.

2.4 Representation of the HOMO state distribution for the isolated NPBA backbone

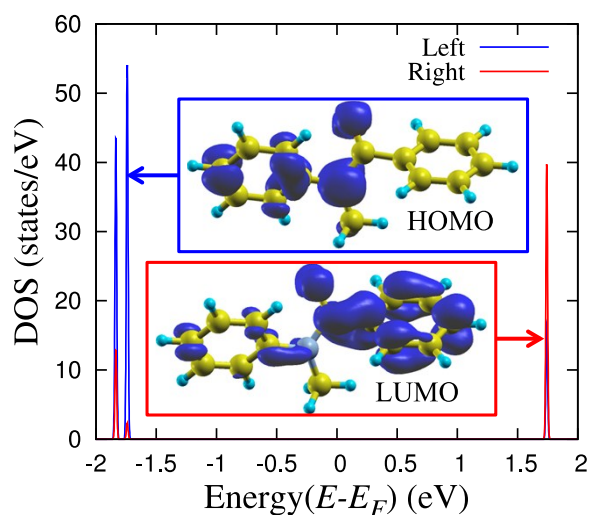


Figure S4. Representation of the density of states of an isolated NPBA molecule determined using GGA-PBE functional as implemented in SIESTA. Insets are LDOS plots for HOMO and LUMO states.

2.5 Single-state tight-binding model

In order to introduce the effect of applying a bias across the molecule, we have used a single-state tight-binding model, as described in details in a previous publication.¹ In this model the molecule is approximated as a single state, coupled to two electron reservoirs (electrodes). For such a system, the transmission function under a certain applied bias, $T(\varepsilon, V)$, can be described by the Breit-Wigner formula:²

$$T(\varepsilon, V) = \frac{4\Gamma_L \Gamma_R}{\left[\varepsilon - \varepsilon_0(V)\right]^2 + (\Gamma_L + \Gamma_R)^2} \quad \text{Eq. S1}$$

where ε_0 is the energy of the isolated state, Γ_L and Γ_R are the left and right coupling to the electrodes, respectively. Based on previous studies,³⁻⁴ low-bias rectification is caused by the energy shifting of the frontier orbital of the molecule; translating into this model, it means that the rectification can be approximated by the asymmetric shifting of ε_0 due to the applied bias. Here, we used the HOMO of the molecule as the single state ε_0 . This state will be spatially localized at the ‘‘centroid’’ of HOMO (see **Figure S5**). The bias-induced shifting of ε_0 is determined by the following equation:

$$\varepsilon_0(V) = \varepsilon_0(0) + V \times \frac{\text{state-lead distance}}{\text{junction length}} \quad \text{Eq. S2}$$

where V is the applied bias. The junction length is the distance between the two gold contacts. The state-lead distance is the distance between the state ε_0 (at the center of mass of HOMO) and the geometric center of the junction in the transport direction. Therefore, the transmission function under different bias can be approximated by substituting **Eq. S2** into **Eq. S1** to give:

$$T(\varepsilon, V) = \frac{4\Gamma_L \Gamma_R}{\left\{ \varepsilon - \left[\varepsilon_0(0) + V \times \frac{\text{state-lead distance}}{\text{junction length}} \right] \right\}^2 + (\Gamma_L + \Gamma_R)^2} \quad \text{Eq. S3}$$

The values of $\varepsilon_0(0)$, Γ_L , and Γ_R can be obtained by fitting the dominant transmission peak using **Eq. S1**, setting these three quantities as parameters. These quantities, together with state-lead distance and junction length, are shown in **Table S1**. As one can see, the RMSE (root-mean-squared error) for all three fits are sufficiently small, indicating less than 1% error between the fitted T and the T calculated as described in the Methods section in main text. Once these parameters are obtained, the transmission function of the dominant transport channel under different biases can be calculated using **Eq. S3**, and in turn the current under those biases by integrating the transmission function. Finally, the rectification ratio can be obtained by taking the ratio of the currents between the positive and negative biases.

Table S1. Parameters from zero-bias transmission function fitted by **Eq. S1**.

Molecule	$\varepsilon_0(0)$ (eV)	Γ_L (eV)	Γ_R (eV)	RMSE (%)	State-lead distance (Å)	Junction length (Å)
CH ₂ -NPBA	-0.286	-0.2304	-0.0091	0.63	3.0192	14.4349
NH ₂ -NPBA	-1.580	-0.0298	-0.0008	0.14	1.2623	14.3949
C ₂ H ₄ -NPBA	-1.110	-0.0322	-0.0024	0.12	0.5187	17.6785

Note: the Gamma values (Γ_L , Γ_R) obtained indicate an asymmetric coupling of the molecular state (gateway orbital) with the leads, which is translated into TF peaks that attain only fractional values of the quantum unit of conductance.

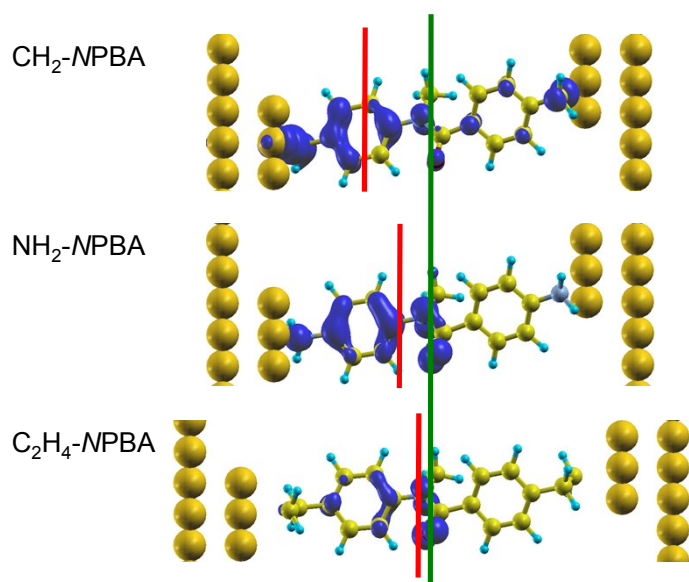


Figure S5. Representation of the isosurfaces of the LDOS for CH₂-NPBA, NH₂-NPBA, and C₂H₄-NPBA at E_{NPBA} . The green and red lines are the projections of the planes that are perpendicular to the transport direction and that include the geometric center of the junction, and the centroid of the HOMO-derived electronic state, respectively.

2.6 Angular dependence of the projected density of states of the phenyl and the Anchor-leads fragments $\text{PDOS}_{\text{Ph}}/\text{PDOS}_{\text{Au-Anchor}}$

To quantify the effects of the different anchoring groups on the electronic coupling between the gold leads and the π -system of the NPBA backbone, we calculated the ratio of the projected density of states (PDOS) of the phenyl fragment (PDOS_{Ph}) to the adjacent lead–anchor motif ($\text{PDOS}_{\text{Au-Anchor}}$) for both **CH₂-NPBA** and **NH₂-NPBA**, with different dihedral angles between the Au–anchor and phenyl ring (see **Figure S6**, which uses **NH₂-NPBA** as an example). We considered rotations of the phenyl plane by +0°, +30°, +60° and +90° relative to the initial (equilibrium) geometry. The density of states distribution is different for **CH₂-NPBA** and **NH₂-NPBA**, therefore, for a fair comparison, the ratio $\text{PDOS}_{\text{Ph}}/\text{PDOS}_{\text{Au-Anchor}}$ calculated for the molecules with same anchoring groups are normalized to the lowest value within the series. In the case of **CH₂-NPBA**, the normalization factor is the ratio obtained for the equilibrium geometry (+0°), while in the case of **NH₂-NPBA**, it is the ratio calculated with an increment of +60° relative to the equilibrium geometry. The results are shown in **Table S2** and **Figure S7**. As can be seen, the PDOS ratio changes dramatically in the case of **CH₂-NPBA**, with a 7-fold increase of the normalized value, within the series. Meanwhile, the PDOS ratio for **NH₂-NPBA** only exhibits a 2-fold decrease through the series.

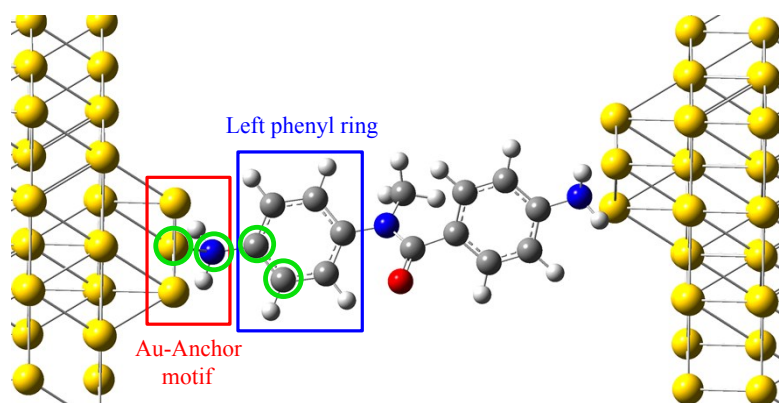


Figure S6. Definition of the regions named Au–Anchor motif and left phenyl ring. The dihedral angle between the Au–anchor and phenyl ring is defined by the atoms labeled with the green circles in the figure. The figure depicts the initial geometry of the NPBA in the junction (+ 0°).

Table S2. PDOS ratios between left phenyl ring and the anchor–Au motif ($\text{PDOS}_{\text{Ph}}/\text{PDOS}_{\text{Au-Anchor}}$), after rotation of phenyl ring plane from its original position by the specified angular increment.

Molecule	+ 0°	+ 30°	+ 60°	+ 90°
CH ₂ -NPBA	1.00	2.52	4.64	7.19
NH ₂ -NPBA	1.74	1.20	1.00	1.00

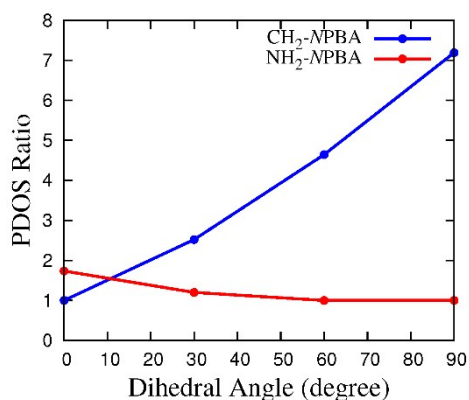
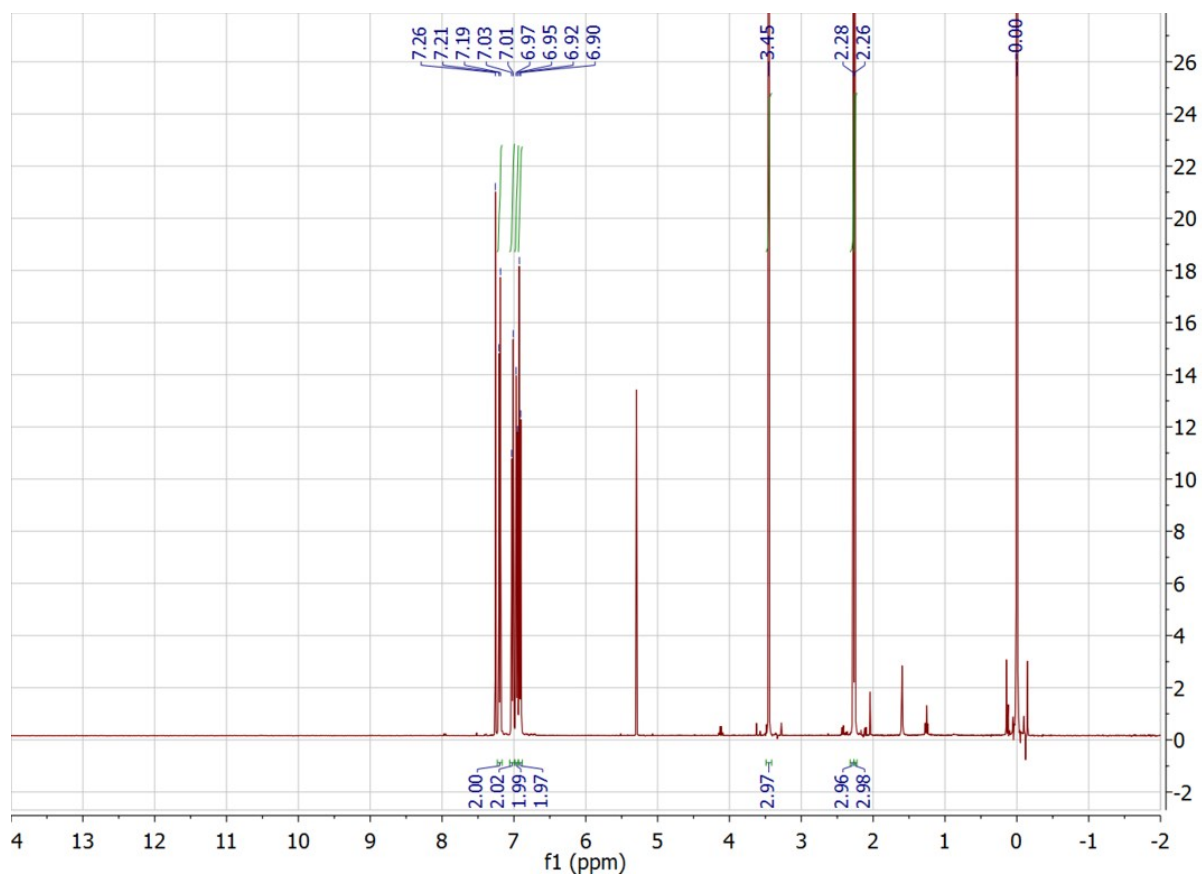


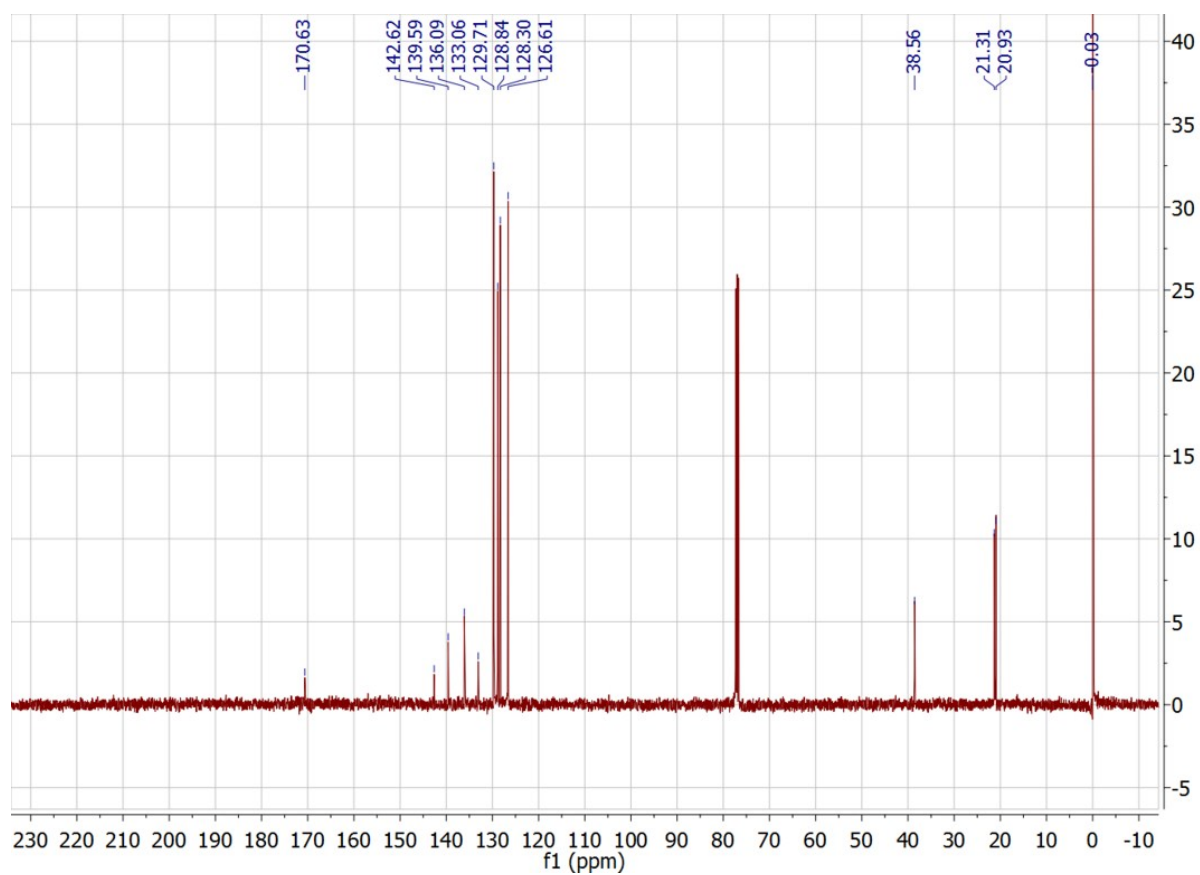
Figure S7. Evolution of the ratio $\text{PDOS}_{\text{Ph}}/\text{PDOS}_{\text{Au-Anchor}}$ as a function of the dihedral angle between the left phenyl ring and the anchor–Au motif for CH₂-NPBA and NH₂-NPBA. The values indicated (+0°, +30°, +60°, +90°) correspond to the incremental rotation of the phenyl ring plane from its original (relaxed) position.

3. NMR spectra

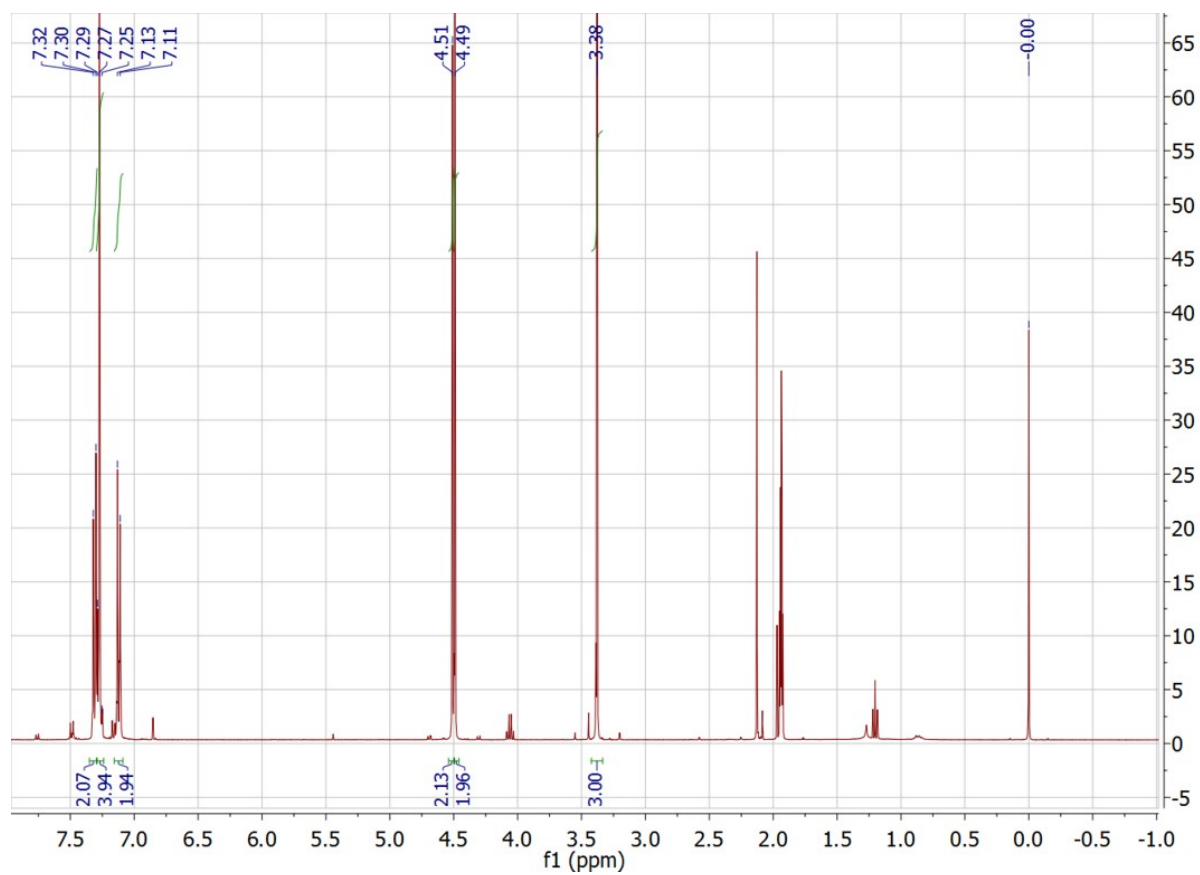
3.1 ^1H NMR spectra of 4'-methyl-N-methyl-N-(4-tolyl)benzamide in CDCl_3



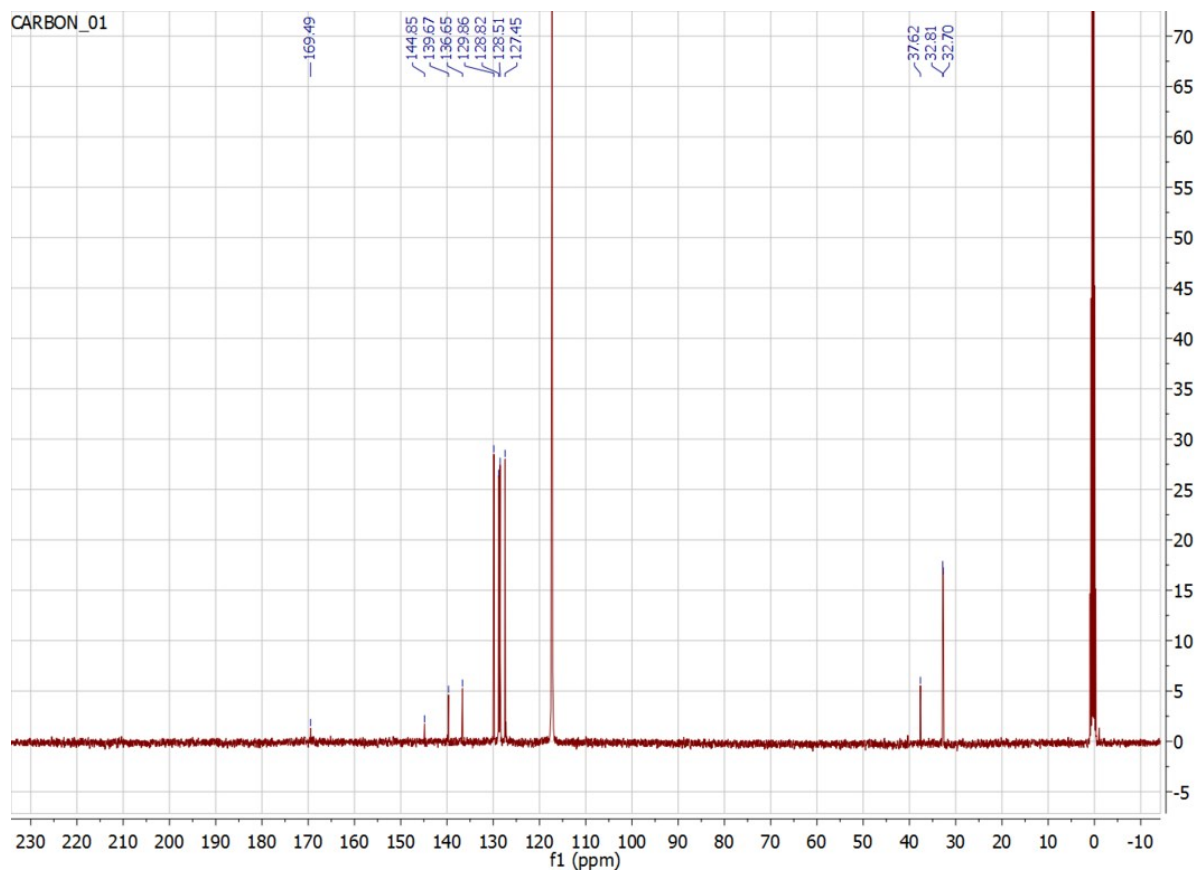
3.2 ^{13}C NMR spectra of 4'-methyl-N-methyl-N-(4-tolyl)benzamide in CDCl_3



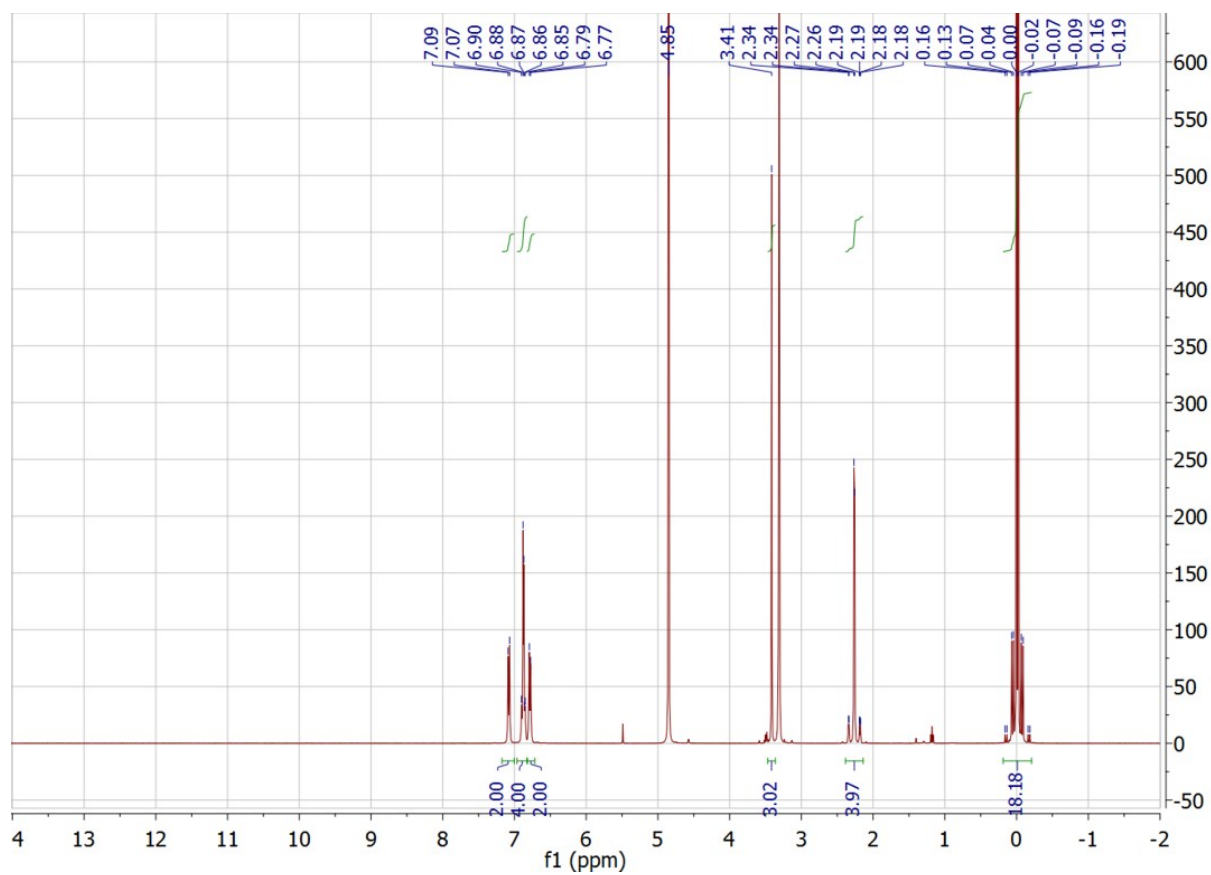
3.3 ^1H NMR spectra of 4'-bromomethyl-*N*-methyl-*N*-[4-(bromomethyl)phenyl]benzamide in CD_3CN



3.4 ^{13}C NMR spectra of 4'-bromomethyl-*N*-methyl-*N*-[4-(bromomethyl)phenyl]benzamide in CD_3CN

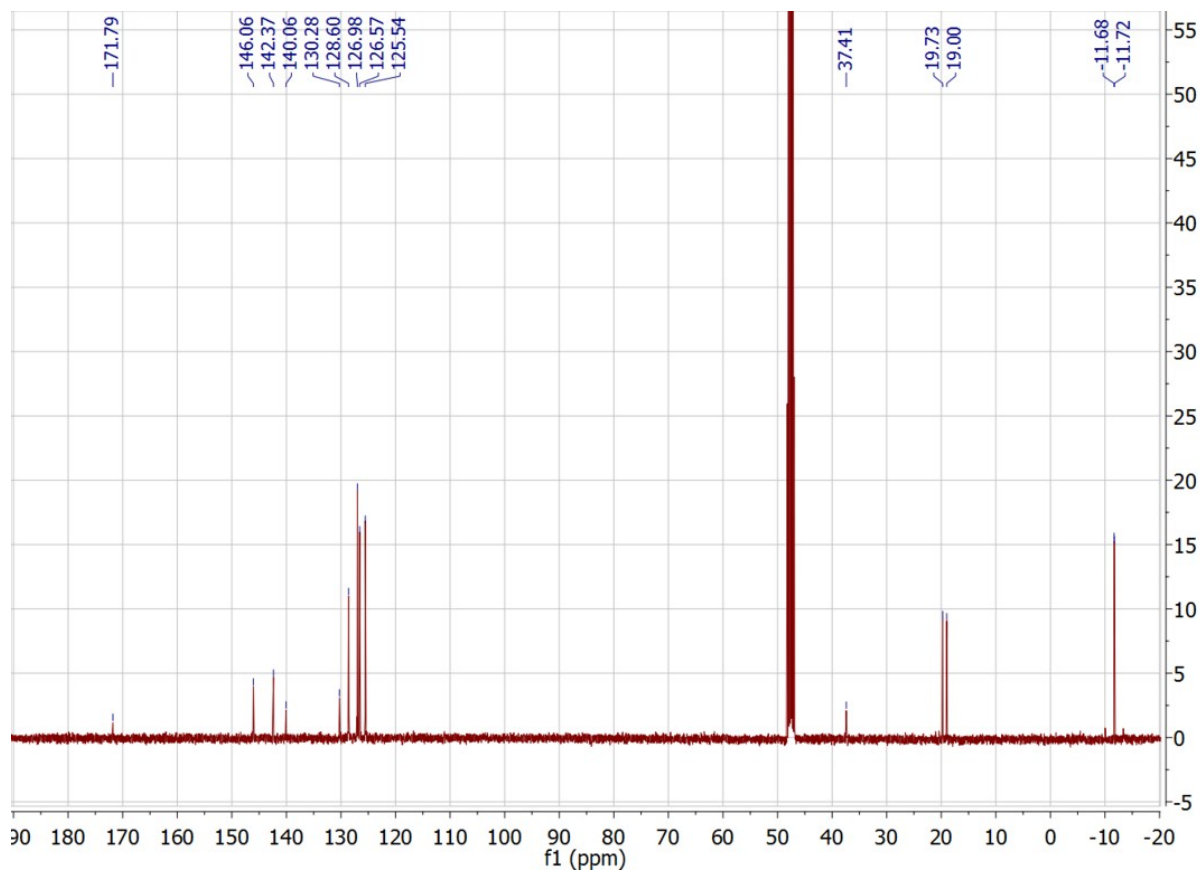


3.5 ^1H NMR spectra of 4'-(trimethylstannyl)methyl-*N*-methyl-*N*-[4((trimethylstannyl)methylphenyl)]benzamide in CD_3OD

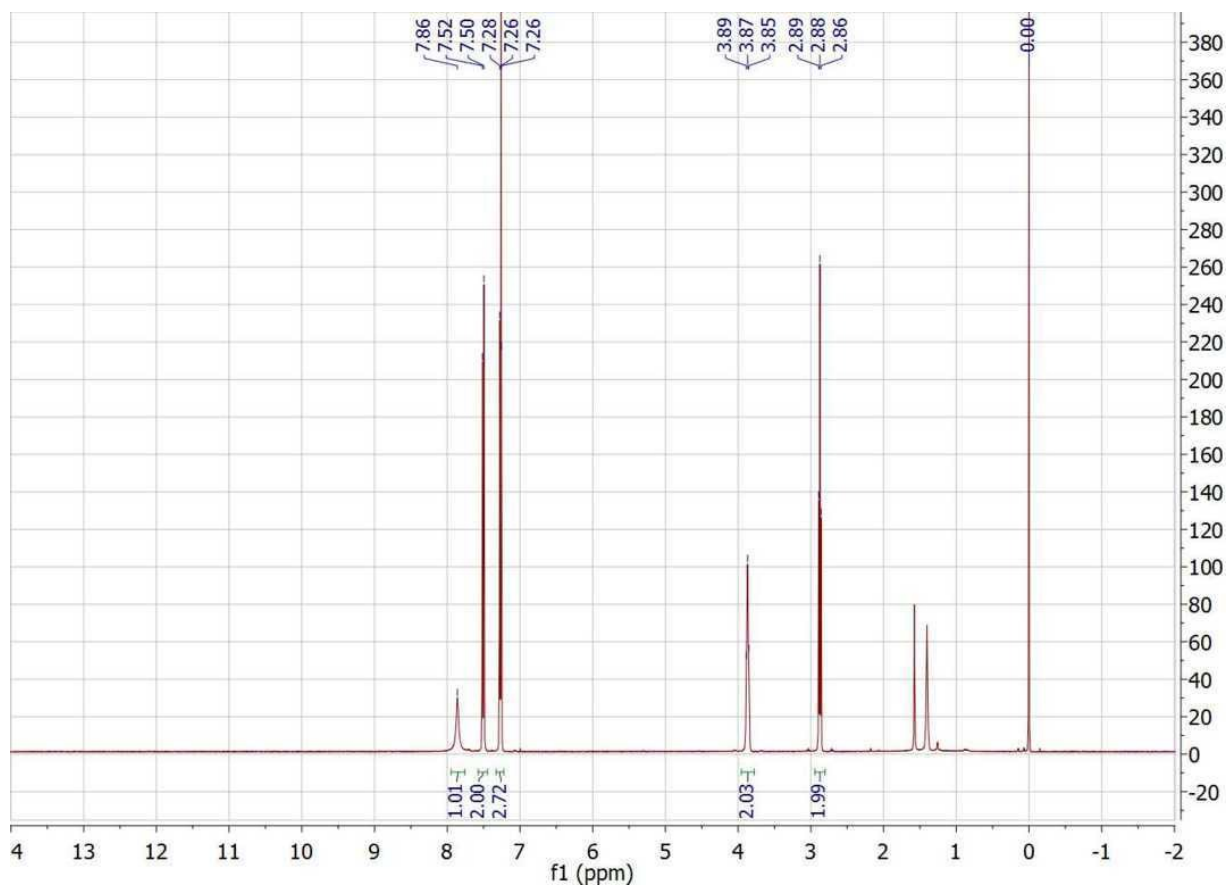


Residual solvent peaks (δ , ppm): CHD_2OD (3.31), H_2O (4.85), CHDCl_2 (5.49)

3.6 ^{13}C NMR spectra of 4'-(trimethylstannyl)methyl-*N*-methyl-*N*-[4((trimethylstannyl)methylphenyl)]benzamide in CD_3OD

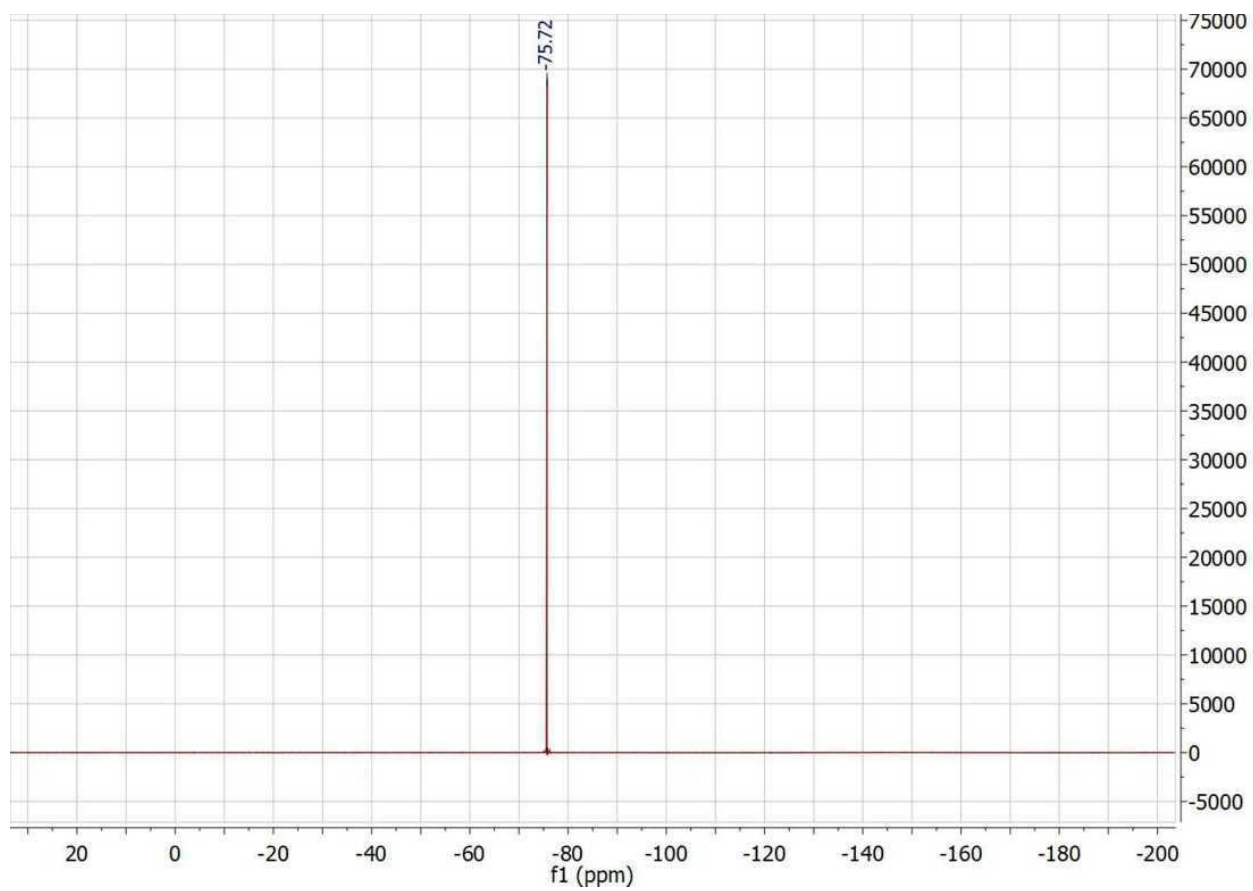


3.7 ^1H NMR spectra of 2[-4-(2',2',2'-trifluoroacetamido)phenyl]ethan-1-ol in CDCl_3

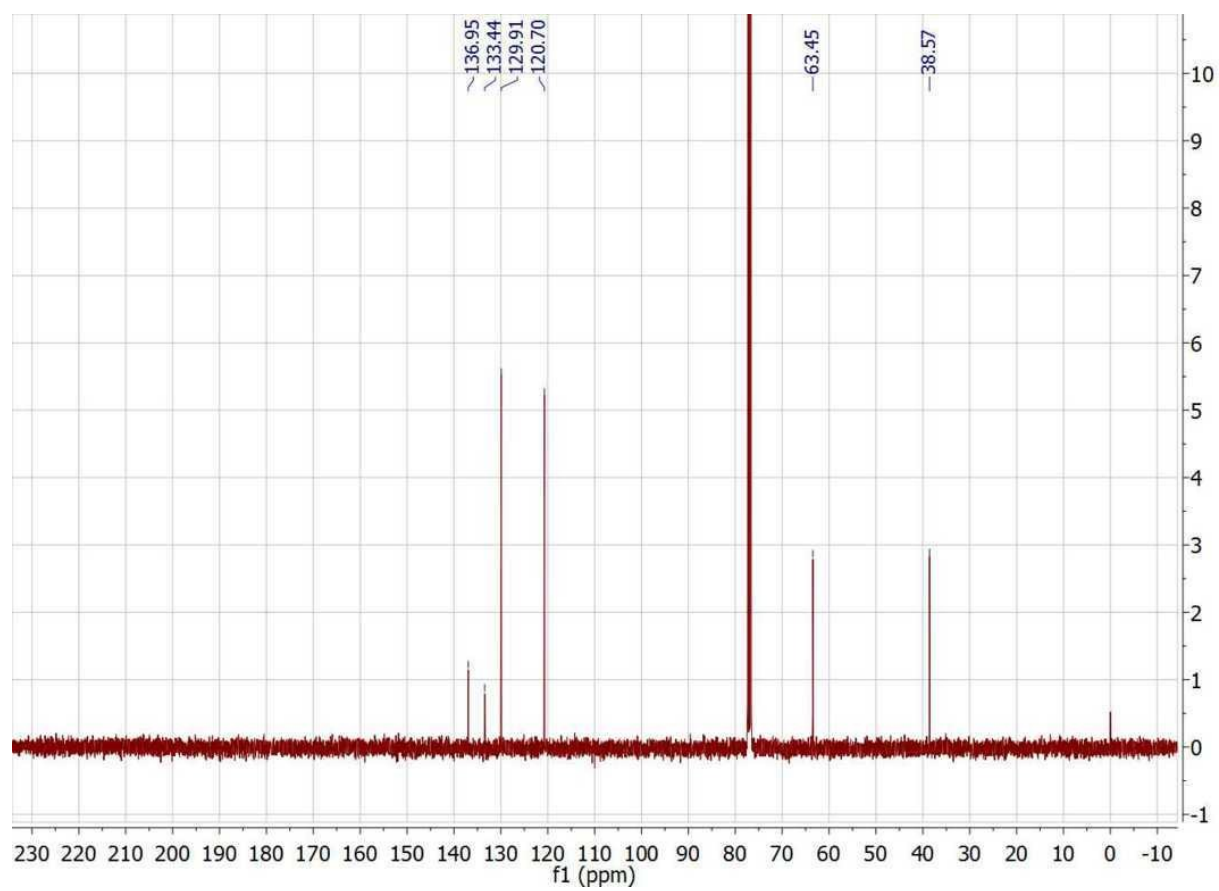


Residual solvent peaks (δ , ppm): CHCl_3 (7.26), H_2O (1.51)

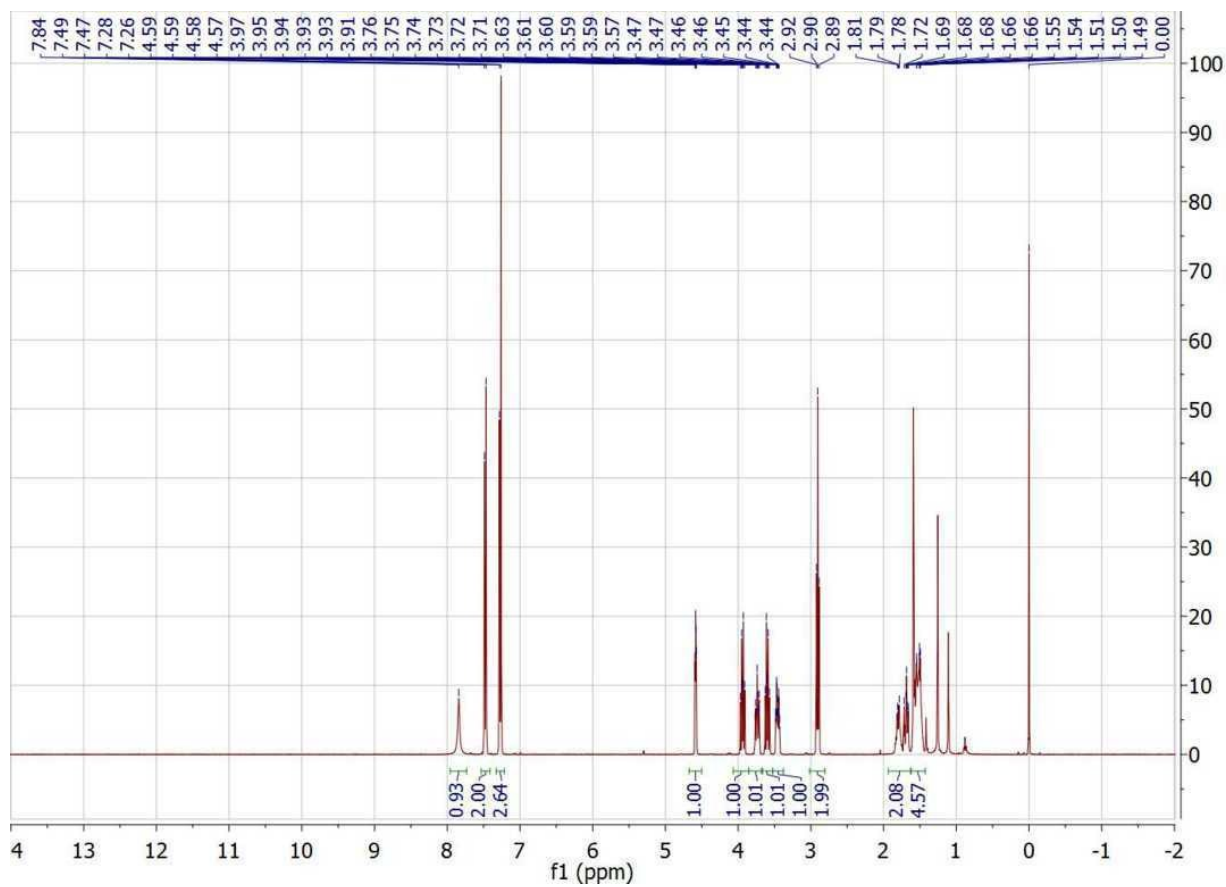
3.8 ^{19}F NMR spectra of 2[-4-(2',2',2'-trifluoroacetamido)phenyl]ethan-1-ol in CDCl_3



3.9 ^{13}C NMR spectra of 2[-4-(2',2'',2''-trifluoroacetamido)phenyl]ethan-1-ol in CDCl_3

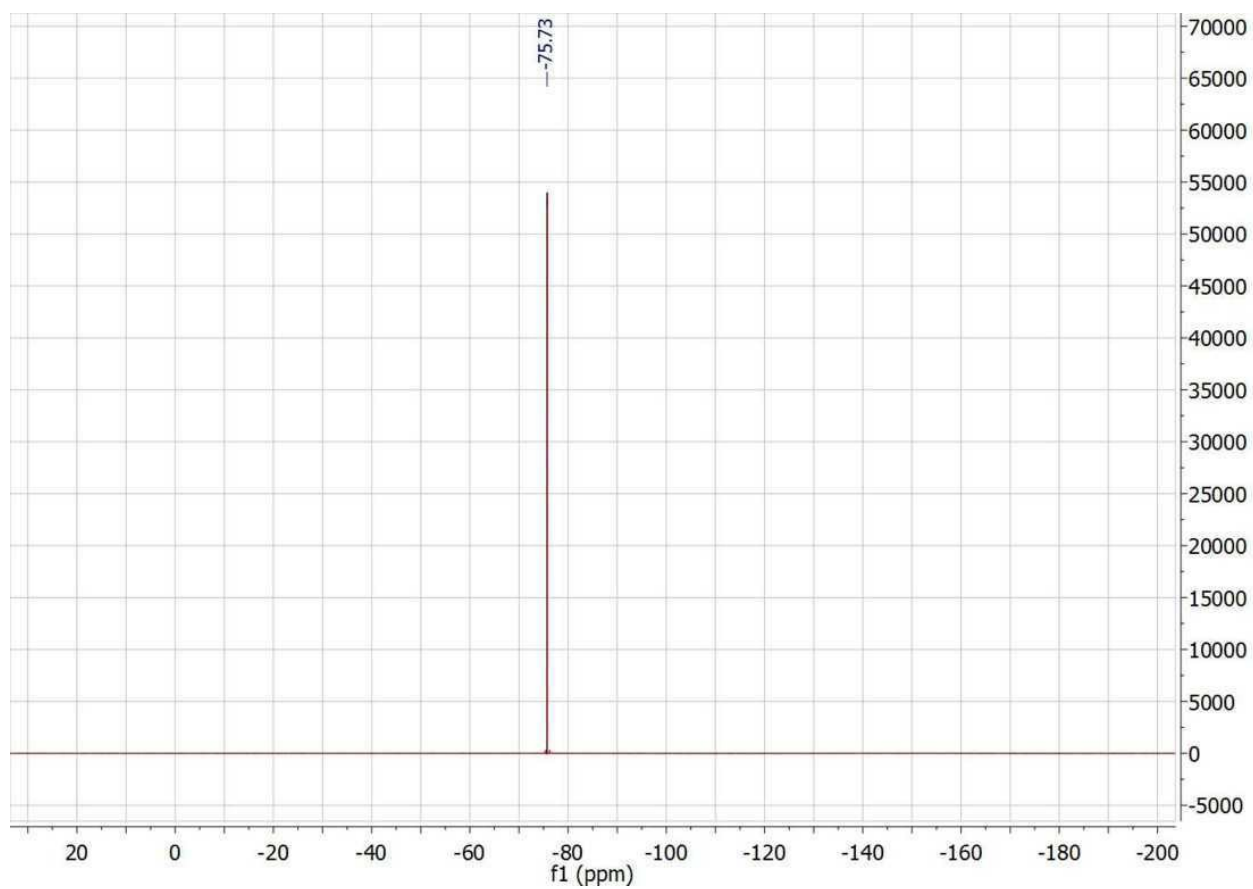


3.10 ¹H NMR spectra of 2,2,2-trifluoro-(4-(2-((tetrahydro-2H-pyran-2-yl)oxy)ethyl)phenyl)acetamide in CDCl₃

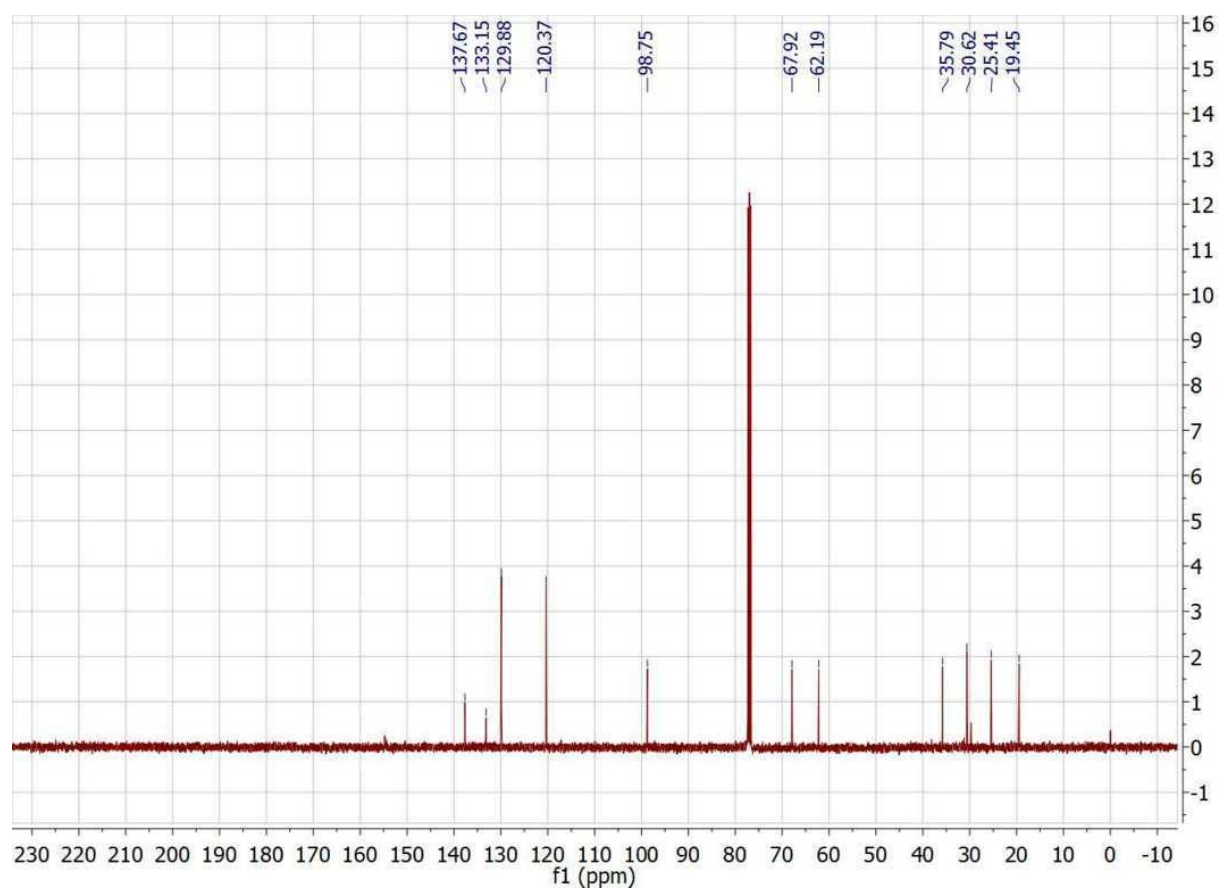


Residual solvent peaks (δ , ppm): CHCl₃ (7.26), H₂O (1.51)

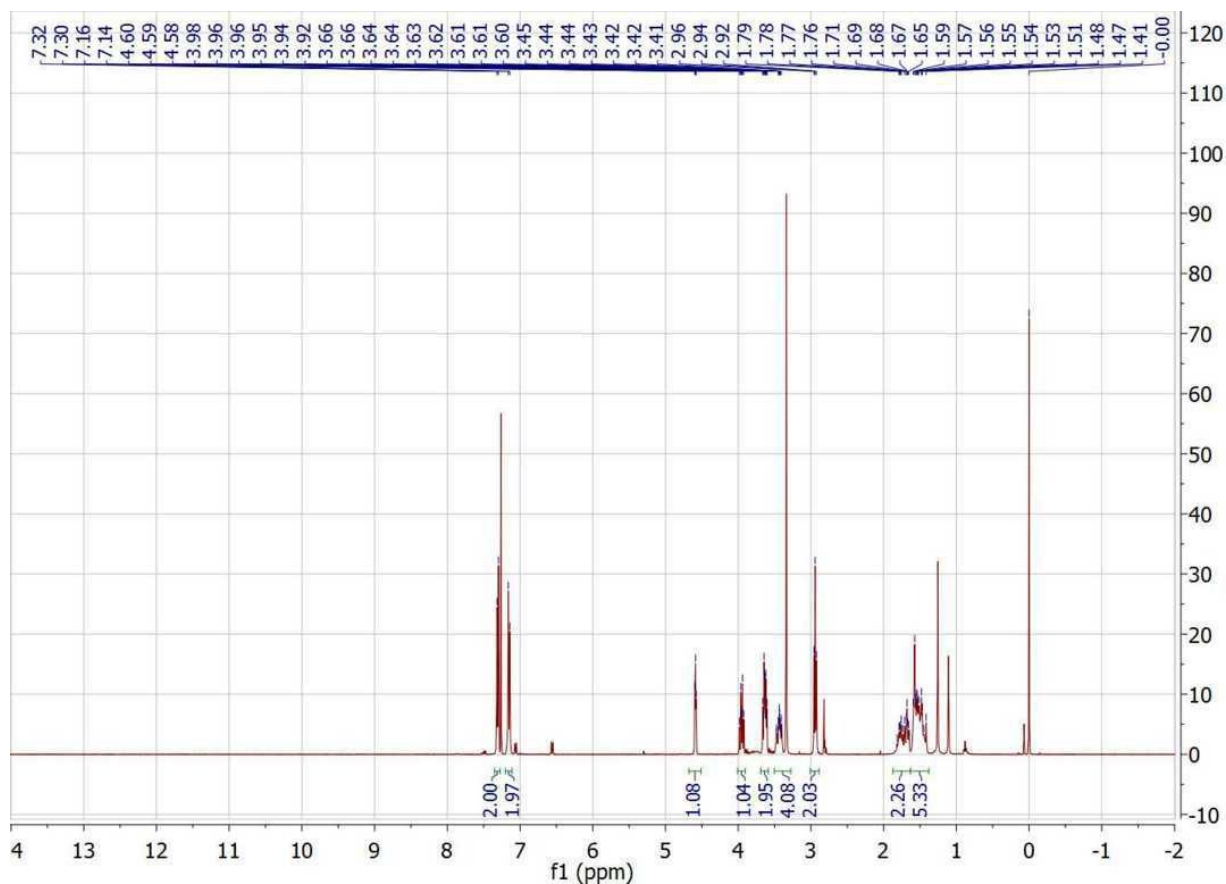
3.11 ^{19}F NMR spectra of 2,2,2-trifluoro-4-(2-((tetrahydro-2*H*-pyran-2-yl)oxy)ethyl)phenyl acetamide in CDCl_3



3.12 ^{13}C NMR spectra of 2,2,2-trifluoro-(4-(2-((tetrahydro-2*H*-pyran-2-yl)oxy)ethyl)phenyl acetamide in CDCl_3

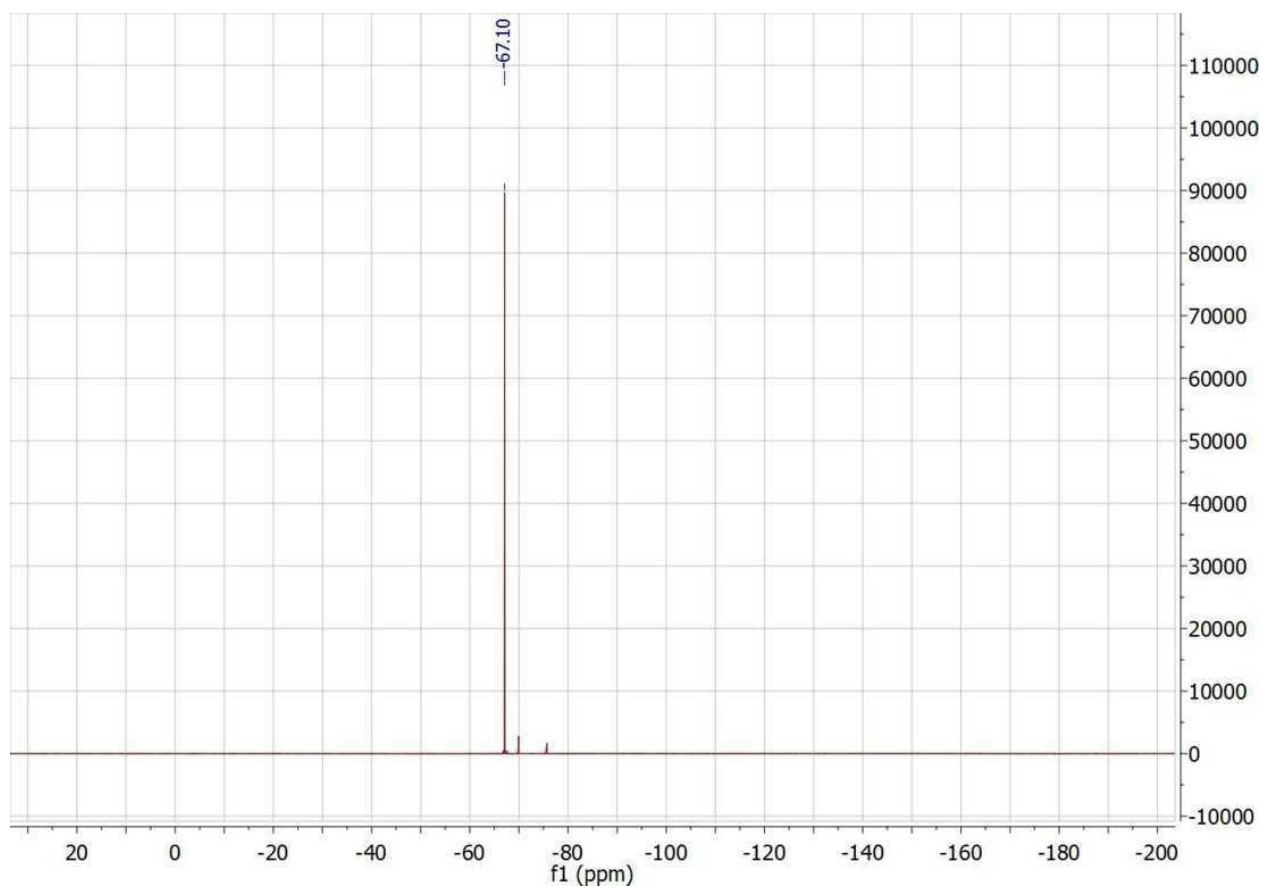


3.13 ^1H NMR spectra of 2,2,2-trifluoro-*N*-methyl-(4-(2-((tetrahydro-2*H*-pyran-2-yl)oxy)ethyl)-phenylacetamide in CDCl_3

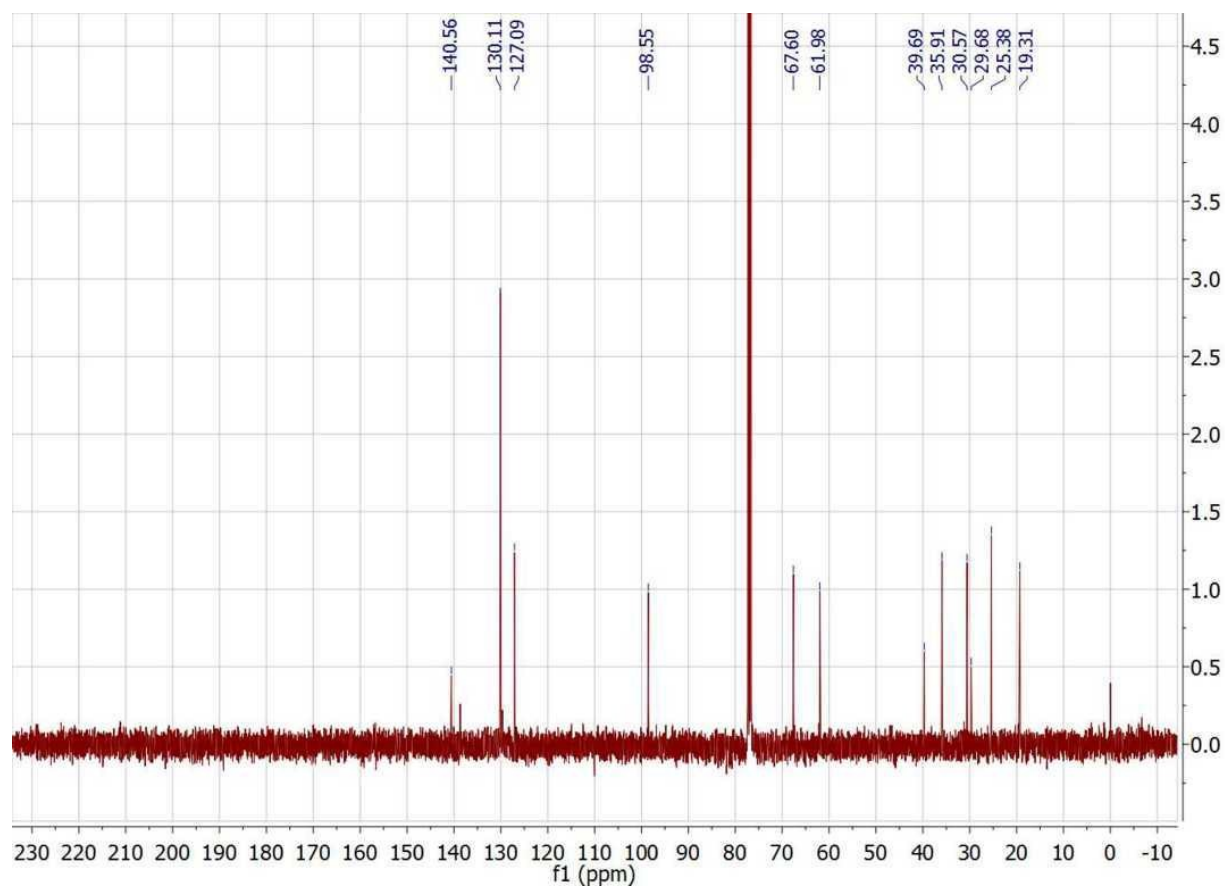


Residual solvent peaks (δ , ppm): CHCl_3 (7.26), H_2O (1.51)

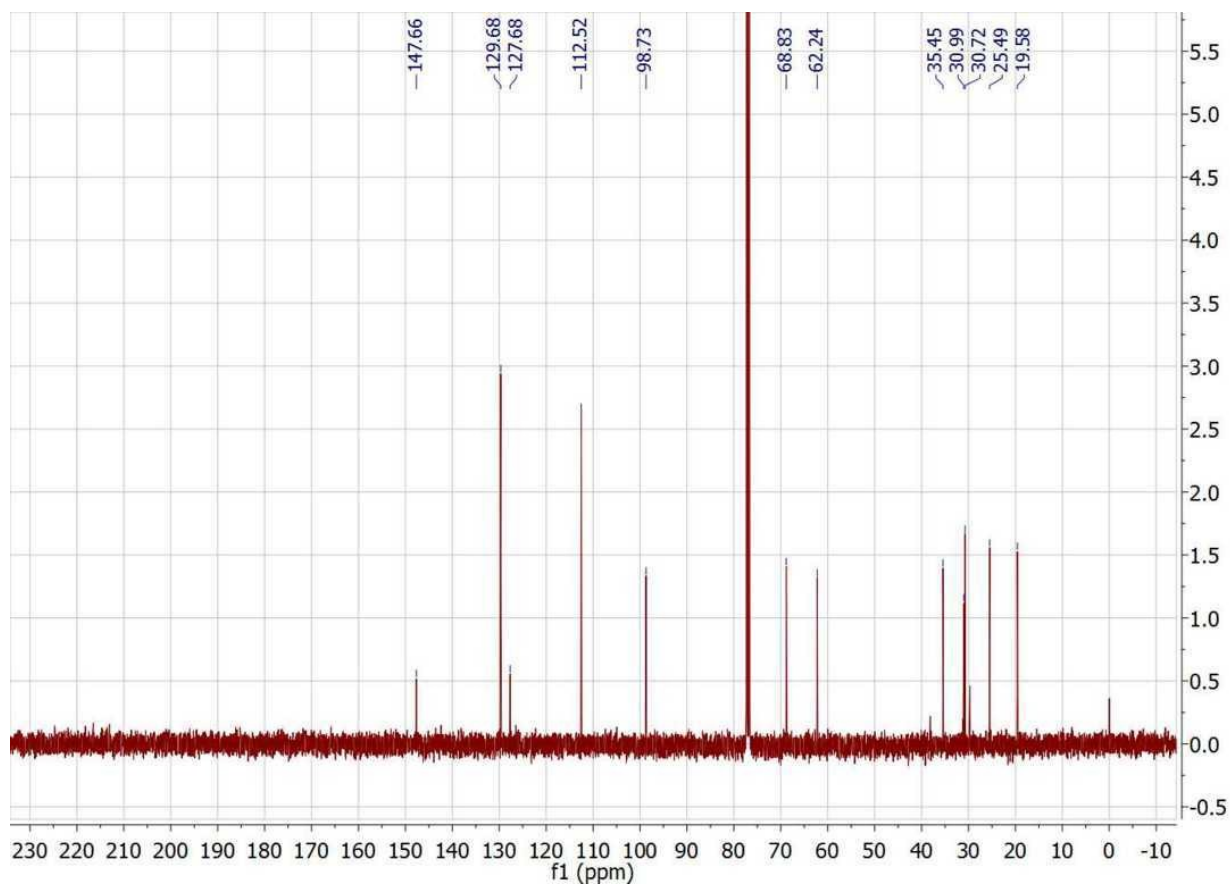
3.14 ^{19}F NMR spectra of 2,2,2-trifluoro-*N*-methyl-(4-(2-((tetrahydro-2*H*-pyran-2-yl)oxy)ethyl)-phenylacetamide in CDCl_3



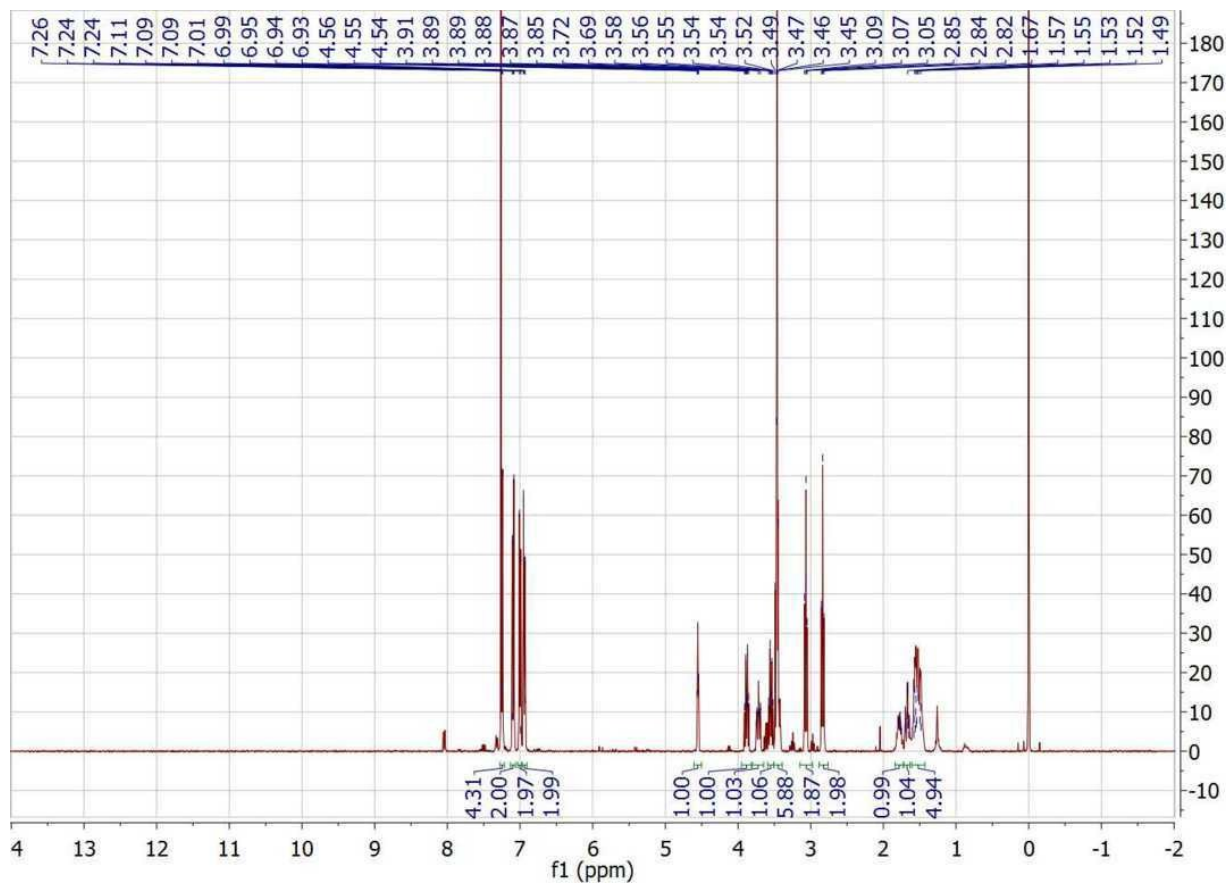
3.15 ^{13}C NMR spectra of 2,2,2-trifluoro-*N*-methyl-(4-(2-((tetrahydro-2*H*-pyran-2-yl)oxy)ethyl)-phenylacetamide in CDCl_3



3.17 ^{13}C NMR spectra of *N*-methyl-(4-(2-((tetrahydro-2*H*-pyran-2-yl)oxy)ethyl)aniline in CDCl_3

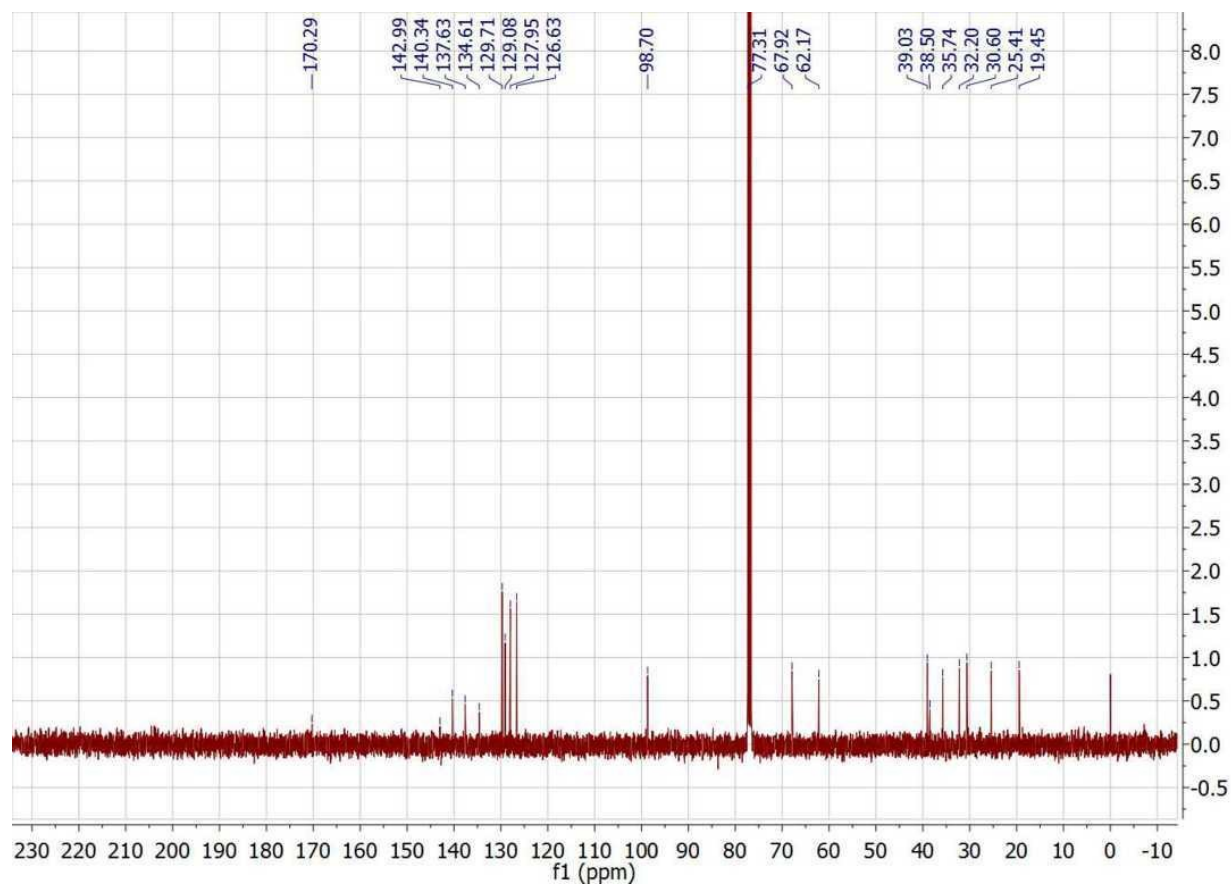


3.18 ^1H NMR spectra of 4-(2-bromoethyl)-*N*-methyl-*N*-(4-(2-((tetrahydro-2*H*-pyran-2-yl)oxy)-ethyl)phenyl)benzamide in CDCl_3

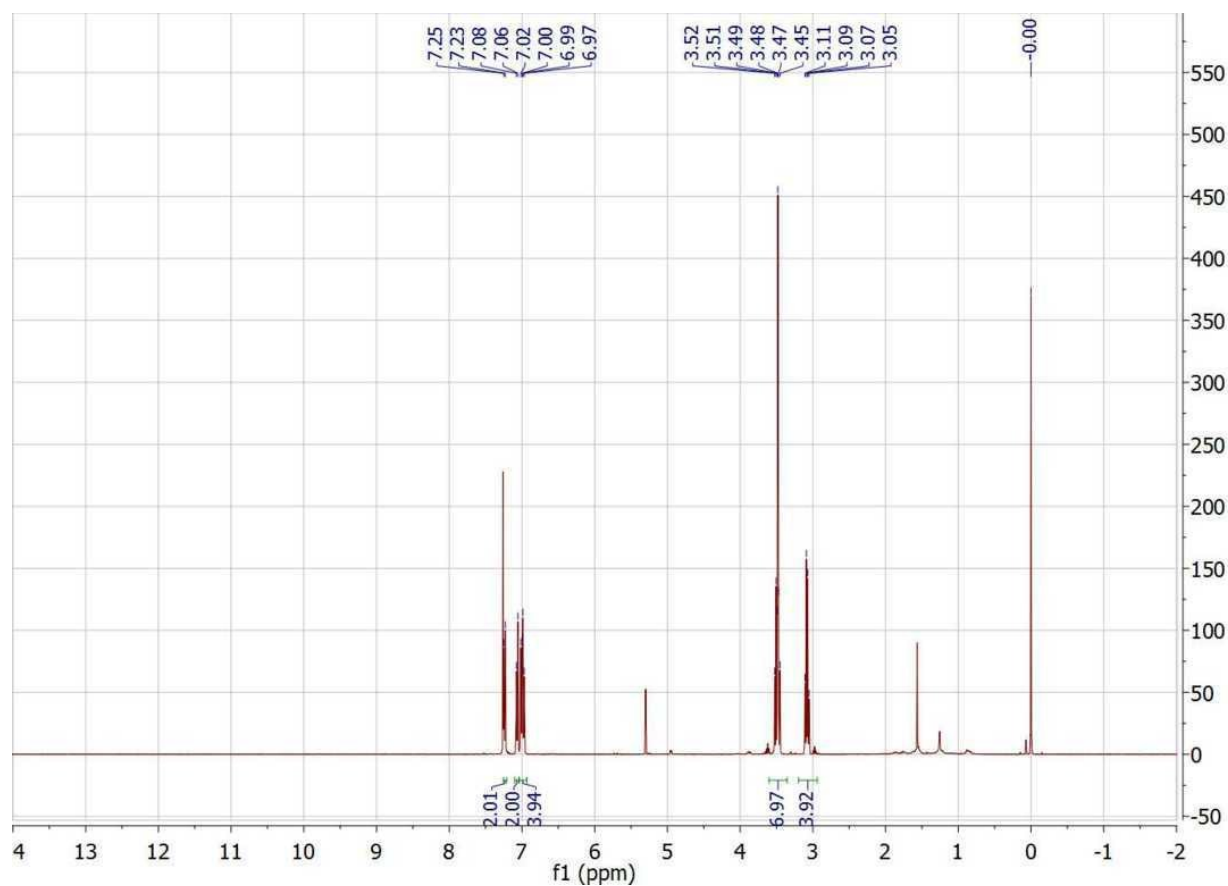


Residual solvent peaks (δ , ppm): CHCl_3 (7.26), H_2O (1.51)

3.19 ^{13}C NMR spectra of 4-(2-bromoethyl)-*N*-methyl-*N*-(4-(2-((tetrahydro-2*H*-pyran-2-yl)oxy)-ethyl)phenyl)benzamide in CDCl_3

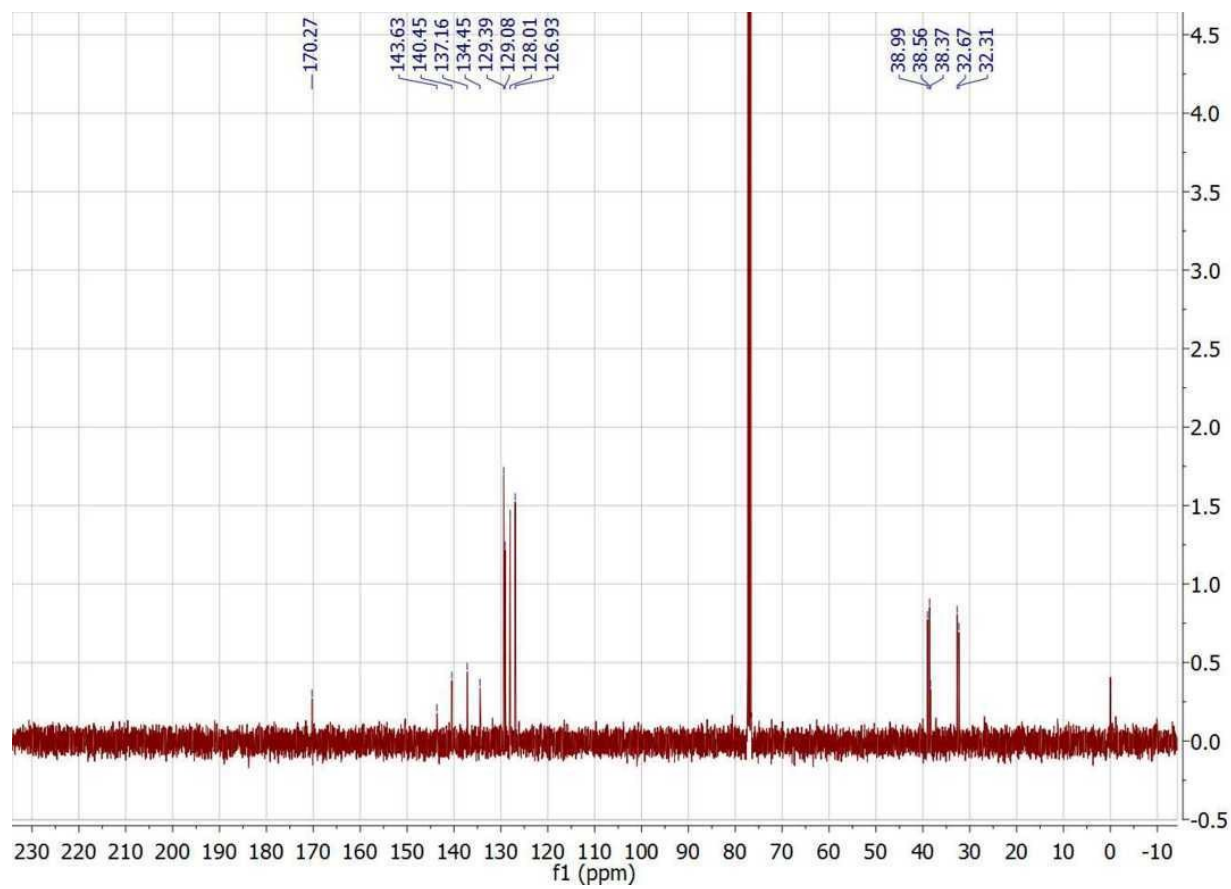


3.20 ^1H NMR spectra of 4-(2-bromoethyl)-*N*-methyl-*N*-(4-(2-bromoethyl)phenyl)benzamide in CDCl_3

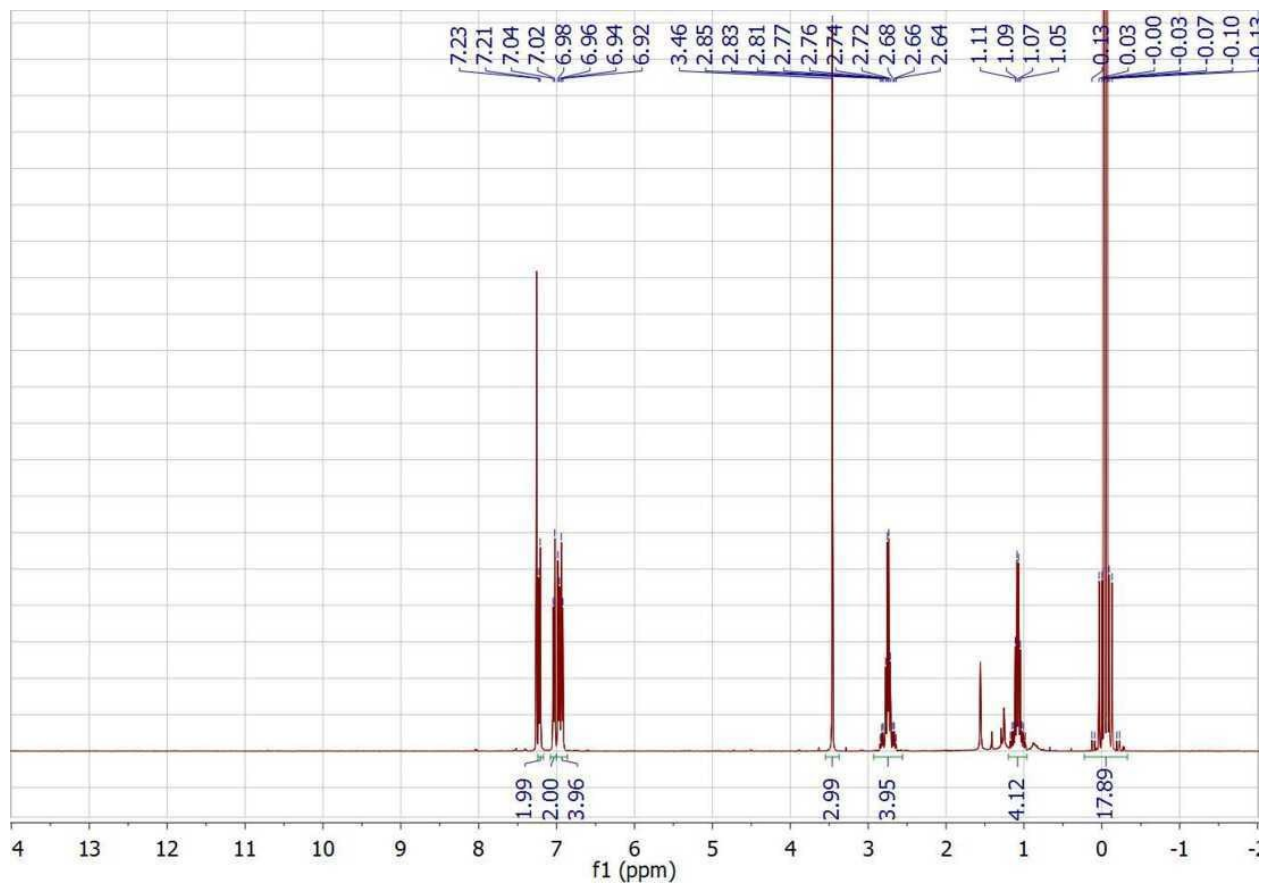


Residual solvent peaks (δ , ppm): CHCl_3 (7.26), H_2O (1.51)

3.21 ^{13}C NMR spectra of 4-(2-bromoethyl)-*N*-methyl-*N*-(4-(2-bromoethyl)phenyl)benzamide in CDCl_3

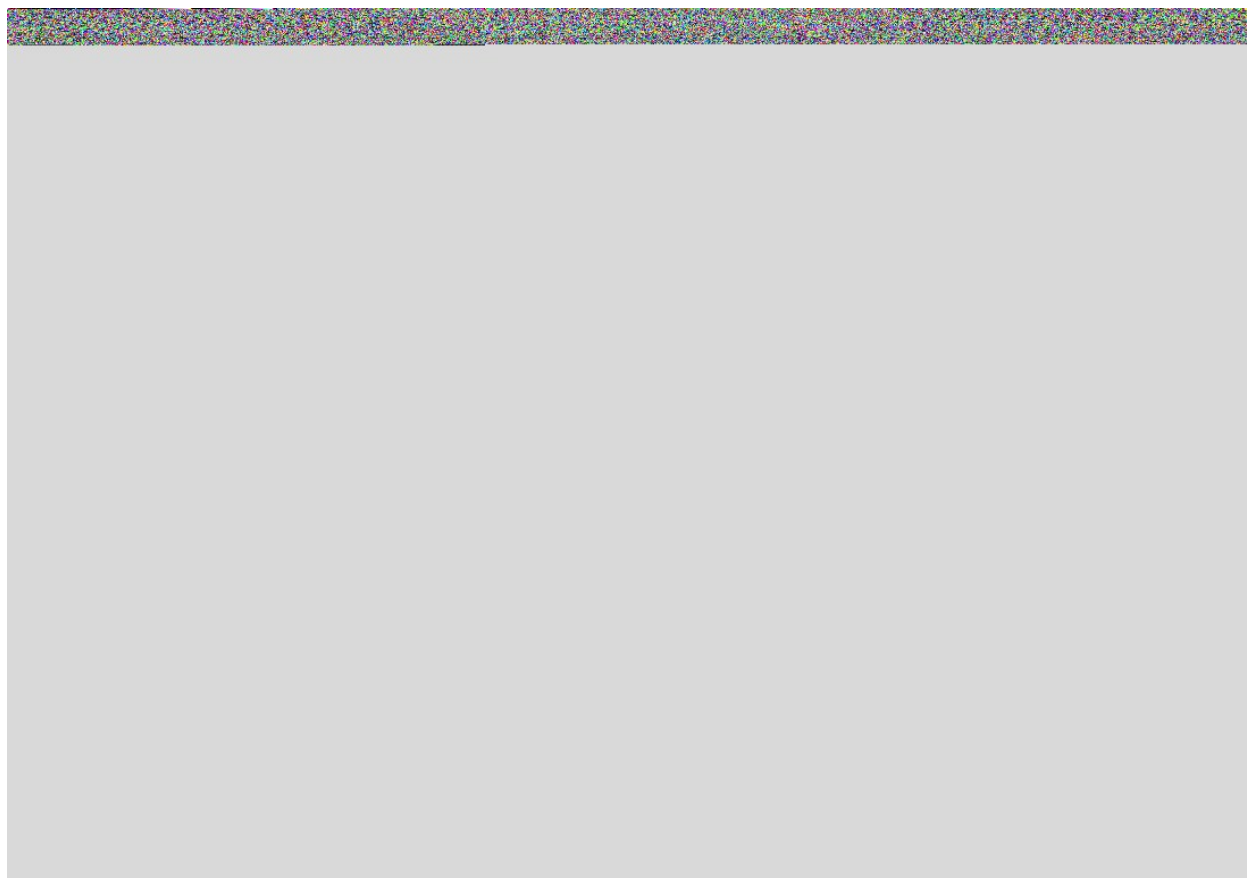


3.22 ^1H NMR spectra of 4-(trimethylstannyl)ethyl-*N*-methyl-*N*-(4((trimethylstannyl)ethyl)-phenyl)benzamide



Residual solvent peaks (δ , ppm): CHCl_3 (7.26), H_2O (1.51)

**3.23 ^{13}C NMR spectra of 4-(trimethylstannyl)ethyl-*N*-methyl-*N*-(4
((trimethylstannyl)ethyl)-phenyl)benzamide**



4. References

1. Koenigsmann, C.; Ding, W.; Koepf, M.; Batra, A.; Venkataraman, L.; Negre, C. F. A.; Brudvig, G. W.; Crabtree, R. H.; Batista, V. S.; Schmittenmaer, C. A. Structure-function relationships in single molecule rectification by N-phenylbenzamide derivatives. *New J Chem* **2016**, *In press* (DOI: 10.1039/C6NJ00870D).
2. Cuveas, J. C.; Elke, S. Nonequilibrium Green's functions formalism. In *Molecular Electronics*, World Scientific Printers: Singapore, 2010; Vol. 1, pp 179-203.
3. Ding, W.; Negre, C. F. A.; Vogt, L.; Batista, V. S. Single Molecule Rectification Induced by the Asymmetry of a Single Frontier Orbital. *Journal of Chemical Theory and Computation* **2014**, *10* (8), 3393-3400.
4. Ding, W.; Koepf, M.; Koenigsmann, C.; Batra, A.; Venkataraman, L.; Negre, C. F. A.; Brudvig, G. W.; Crabtree, R. H.; Schmittenmaer, C. A.; Batista, V. S. Computational Design of Intrinsic Molecular Rectifiers Based on Asymmetric Functionalization of N-Phenylbenzamide. *Journal of Chemical Theory and Computation* **2015**, *11* (12), 5888-5896.